Interplay Between Histone H3 Lysine 56 Deacetylation and Chromatin Modifiers in Response to DNA Damage

Antoine Simoneau,*,[1] Neda Delgoshaie,†,[1] Ivana Celic,‡ Junbiao Dai,‡,§ Nebiyu Abshiru,†, Santiago Costantino,*,‡‡ Pierre Thibault,†,** Jef D. Boeke,‡,§§ Alain Verreault,†,*** and Hugo Wurtele*,††,[2]**

*Centre de recherche de l'Hôpital Maisonneuve-Rosemont, Montréal, QC, Canada H1T 2M4, †Institute for Research in Immunology and Cancer , ***Département de Pathologie et Biologie Cellulaire, ††Département de Médecine, ‡‡Département d'ophtalmologie, and **Département de Chimie, Université de Montréal, Succursale Centre-Ville, Montreal, QC, Canada H3C 3J7, ‡High Throughput Biology Center, Johns Hopkins University School of Medicine, Baltimore, Maryland 21205, §School of Life Sciences, Tsinghua University, Beijing, China 100084, and §§Institute for Systems Genetics and Department of Biochemistry and Molecular Pharmacology, New York University Langone Medical Center, New York, New York 10016

ABSTRACT In *Saccharomyces cerevisiae*, histone H3 lysine 56 acetylation (H3K56Ac) is present in newly synthesized histones deposited throughout the genome during DNA replication. The sirtuins Hst3 and Hst4 deacetylate H3K56 after S phase, and virtually all histone H3 molecules are K56 acetylated throughout the cell cycle in *hst3*Δ *hst4*Δ mutants. Failure to deacetylate H3K56 causes thermosensitivity, spontaneous DNA damage, and sensitivity to replicative stress via molecular mechanisms that remain unclear. Here we demonstrate that unlike wild-type cells, *hst3*Δ *hst4*Δ cells are unable to complete genome duplication and accumulate persistent foci containing the homologous recombination protein Rad52 after exposure to genotoxic drugs during S phase. In response to replicative stress, cells lacking Hst3 and Hst4 also displayed intense foci containing the Rfa1 subunit of the single-stranded DNA binding protein complex RPA, as well as persistent activation of DNA damage–induced kinases. To investigate the basis of these phenotypes, we identified histone point mutations that modulate the temperature and genotoxic drug sensitivity of *hst3*Δ *hst4*Δ cells. We found that reducing the levels of histone H4 lysine 16 acetylation or H3 lysine 79 methylation partially suppresses these sensitivities and reduces spontaneous and genotoxin-induced activation of the DNA damage-response kinase Rad53 in *hst3*Δ *hst4*Δ cells. Our data further suggest that elevated DNA damage–induced signaling significantly contributes to the phenotypes of *hst3*Δ *hst4*Δ cells. Overall, these results outline a novel interplay between H3K56Ac, H3K79 methylation, and H4K16 acetylation in the cellular response to DNA damage.

KEYWORDS DNA damage repair and checkpoint response; H3 lysine 56 acetylation; H3 lysine 79 methylation; H4 lysine 16 acetylation; chromatin structure

CHROMATIN structure influences major DNA metabolic processes such as transcription, DNA replication, and DNA repair (Wurtele and Verreault 2006; Campos and Reinberg 2009). The basic building block of chromatin is the nucleosome core particle composed of 147 bp of DNA wrapped around the surface of a protein octamer consisting of two molecules each of histones H2A, H2B, H3, and H4. During DNA replication, preexisting (old) histones are segregated onto sister chromatids, while new histones are deposited onto replicated DNA in order to restore normal nucleosome density on nascent sister chromatids (Ransom *et al.* 2010; Li and Zhang 2012). In humans, newly synthesized histones H3 and H4 are acetylated on multiple residues within their N-terminal tails (Ruiz-Carrillo *et al.* 1975; Benson *et al.* 2006; Jasencakova *et al.* 2010) and then are deacetylated following their incorporation into chromatin (Jackson *et al.* 1976;

doi: 10.1534/genetics.115.175919
Manuscript received September 20, 2014; accepted for publication March 12, 2015; published Early Online March 18, 2015.
Supporting information is available online at http://www.genetics.org/lookup/suppl/doi:10.1534/genetics.115.175919/-/DC1
[1]These authors contributed equally to this work.
[2]Corresponding author: Centre de recherche de l'Hôpital Maisonneuve-Rosemont, Montréal, Canada H1T 2M4. E-mail: hugo.wurtele@umontreal.ca

Taddei *et al.* 1999). In the yeast *Saccharomyces cerevisiae* and other fungi, new H3 and H4 molecules are acetylated on their N-terminal tails (Parthun *et al.* 1996; Burgess *et al.* 2010), as well as within their globular domains, notably at histone H4 lysine 91 and H3 lysine 56 (H3K56Ac) (Hyland *et al.* 2005; Masumoto *et al.* 2005; Xu *et al.* 2005; Ye *et al.* 2005; Recht *et al.* 2006). In yeast, H3K56Ac is present in virtually all newly synthesized H3 molecules deposited throughout the genome during S phase (Celic *et al.* 2006) but is much less abundant in preexisting histones (Masumoto *et al.* 2005). H3K56Ac is catalyzed by Rtt109 acetyltransferase in concert with the histone-binding protein Asf1 (Celic *et al.* 2006; Schneider *et al.* 2006; Driscoll *et al.* 2007; Han *et al.* 2007a, b; Tsubota *et al.* 2007), while deacetylation of this residue depends, in a largely redundant manner, on the sirtuins Hst3 and Hst4 (Celic *et al.* 2006; Maas *et al.* 2006; Thaminy *et al.* 2007; Haldar and Kamakaka 2008). Hst3 and Hst4 are absent during S phase, and as a result, H3K56Ac progressively accumulates in nascent chromatin during replication and reaches maximal levels after completion of DNA synthesis (Masumoto *et al.* 2005; Maas *et al.* 2006; Kaplan *et al.* 2008). In the absence of DNA damage, H3K56Ac is then removed genome-wide on induction of Hst3 and Hst4 expression during subsequent G_2/M and G_1 phases (Maas *et al.* 2006).

Hst3 and Hst4 are homologs of Sir2 (Brachmann *et al.* 1995), the founding member of the sirtuin family of nicotinamide adenine dinucleotide (NAD^+)–dependent deacetylases (Imai *et al.* 2000; Landry *et al.* 2000; Smith *et al.* 2000; Tanny and Moazed 2001). Deletion of *HST3* causes mild phenotypes such as elevated frequencies of Rad52 foci and reduced replicative lifespan (Alvaro *et al.* 2007; Dang *et al.* 2009). In striking contrast, cells lacking both *HST3* and *HST4* (*hst3*Δ *hst4*Δ mutants) display extreme sensitivity to genotoxic agents and severe phenotypes that may be related to their inability to respond appropriately to spontaneous DNA damage, including thermosensitivity, reduced viability, mitotic instability, and dramatically reduced replicative lifespan (Brachmann *et al.* 1995; Celic *et al.* 2006; Hachinohe *et al.* 2011). In contrast to *hst3*Δ or *hst4*Δ single mutants, essentially all H3 molecules are K56 acetylated throughout the genome and during the entire cell cycle in the double mutant (Celic *et al.* 2006). Remarkably, many of the aforementioned *hst3*Δ *hst4*Δ–associated phenotypes are strongly attenuated by mutating H3K56 to a nonacetylable arginine residue (Celic *et al.* 2006; Maas *et al.* 2006). This suggests that H3K56 hyperacetylation and/or the constitutive presence of H3K56Ac throughout the cell cycle is the root cause of the severe phenotypes observed in *hst3*Δ *hst4*Δ mutants. In support of this, our previously published mass spectrometry data indicate that among several sites of acetylation in H3/H4, only H3K56Ac exhibited a striking increase in acetylation stoichiometry in *hst3*Δ *hst4*Δ mutants (Drogaris *et al.* 2008), illustrating the remarkable *in vivo* substrate selectivity of Hst3 and Hst4.

Accumulating evidence indicates that the yeast chromosome acetylation-deacetylation cycle is critical for efficient cellular responses to DNA damage. Indeed, both acetylation and, to an even greater extent, deacetylation of H3K56 promote cell survival in response to spontaneous or genotoxic agent–induced DNA lesions (Hyland *et al.* 2005; Masumoto *et al.* 2005; Ozdemir *et al.* 2005; Celic *et al.* 2006; Maas *et al.* 2006; Recht *et al.* 2006; Alvaro *et al.* 2007; Wurtele *et al.* 2010, 2012; Reid *et al.* 2011). The molecular mechanisms by which lack of or excess H3K56Ac causes cellular sensitivity to DNA damage are poorly understood. H3K56Ac promotes efficient chromatin assembly during DNA replication at least in part by enhancing the affinity of nucleosome assembly factors for newly synthesized H3 molecules (Li *et al.* 2008; Su *et al.* 2012). H3K56Ac also promotes efficient flow of newly synthesized histones between histone chaperones by facilitating transient ubiquitination of histone H3 by the Rtt101-Mms1-Mms22 ubiquitin ligase complex (Han *et al.* 2013). Such ubiquitination events are believed to release new histones from Asf1, thereby increasing the availability of free histones for downstream chaperones (Han *et al.* 2013). However, as a result of DNA damage–induced Hst3 degradation (Thaminy *et al.* 2007; Haldar and Kamakaka 2008), K56-acetylated H3 molecules incorporated into chromatin retain their acetylation until DNA damage has been repaired (Masumoto *et al.* 2005). In addition, several distinct mutations suppress the phenotypes of *hst3*Δ *hst4*Δ cells without modulating H3K56Ac levels, suggesting that abnormal persistence of H3K56Ac throughout the cell cycle may cause defects in processes linked to DNA replication and repair (Collins *et al.* 2007; Celic *et al.* 2008). However, the putative functions of K56-acetylated H3 molecules incorporated in chromatin remain poorly characterized. Here we further investigated the basis of the phenotypes caused by H3K56 hyperacetylation in yeast and identified a novel feature of the yeast DNA damage response, namely, a functional cross talk between H3K56Ac and two other abundant histone post-translational modifications: histone H3 lysine 79 methylation and H4 lysine 16 acetylation.

Materials and Methods

Strains, plasmids, and growth conditions

Plasmids pJP11 (p*CEN LYS2 HHT1-HHF1* and p*CEN-URA3-HST3*) (pRS416-based) were described previously (Park *et al.* 2002; Celic *et al.* 2006) . The pEMH-based plasmids encoding *HHT2-HHF2* gene mutations (p*CEN TRP1 HHT2-HHF2*) were described previously (Hyland *et al.* 2005). Tagging of the *CDC45* gene with a C-terminal triple HA epitope was achieved by transformation of *Nco*I-linearized pRS405-CDC45-HA/C (Aparicio *et al.* 1997) and selection of Leu^+ colonies where the epitope tagging vector was integrated at the *CDC45* locus. *MAT**a***- and *MATα*-expressing plasmids were described previously (Barbour and Xiao 2006).

All the strains used in this work are described in Table 1. They were generated by standard methods and grown under standard conditions unless otherwise stated. Strain ICY1345 was used to assess the phenotypes caused by introducing histone H3/H4 gene mutations in cells carrying *HST3* and

HST4 gene deletions (Table 2 and Table 3). pEMH7-based plasmids (*CEN TRP1 HHT2-HHF2*) that carried H3 or H4 mutations were transformed into ICY1345, and Ura$^+$ Lys$^+$ Trp$^+$ transformants were selected. The Lys$^+$ pJP11 plasmid encoding wild-type (WT) H3 and H4 was selected against on α-aminoadipic acid plates, resulting in Lys$^-$ strains lacking the plasmid encoding WT H3 and H4 genes (Ito-Harashima and McCusker 2004). To test whether specific H3 or H4 gene mutations were able to suppress the phenotypes of *hst3*Δ *hst4*Δ mutants, the aforementioned strains were plated on synthetic complete solid medium without tryptophan (SC-Trp medium) containing 5-fluoroorotic acid (5-FOA) at different temperatures. 5-FOA was used to select against the p*CEN-URA3-HST3* plasmid (Celic *et al.* 2006). Selection against the *HST3* plasmid to uncover *hst3*Δ *hst4*Δ phenotypes was performed immediately before phenotypic analysis because long-term propagation of *hst3*Δ *hst4*Δ mutants leads to the emergence of spontaneous suppressors and genome rearrangements (Brachmann *et al.* 1995).

Isolation of independent spontaneous suppressors of the temperature-sensitivity phenotype of hst3Δ hst4Δ cells

A similar strategy was used to isolate spontaneous suppressors of *hst3*Δ *hst4*Δ mutants. Strain ICY703 (Table 1) was used as a starting point to identify spontaneous suppressors of the temperature-sensitive (Ts-) phenotype. ICY703 contains chromosomal deletions of the *HST3* and *HST4* genes that are covered by a p*CEN-URA3-HST3* plasmid. Independent cultures of ICY703 were plated on 5-FOA plates at 37°. One temperature-resistant (Tr) colony per independent culture of ICY703 was streaked onto a second 5-FOA plate at 37° to isolate single colonies that were temperature and 5-FOA resistant. Those independent suppressor strains were tested by PCR to verify that the *HST3* gene was absent from the thermoresistant strains. The PCR primers chosen for this test amplify a 670-bp DNA fragment derived from the 3′ end of *HST3*. The forward primer was Hst3-C (5′-GTCACATTTCTTGAATCC CAAATAC), and the reverse primer was Hst3-D (5′-TTTGTAG ACTGTTAAAGAGCCATCC).

Cell synchronization, transient treatment with genotoxic agents, and cell viability assays

Cells were grown overnight in YPD medium at 25° and arrested in G_1 using 5 μg/ml α-factor for 90 min, followed by the addition of a second dose of α-factor at 5 μg/ml for 75 min. Cells were then released into the cell cycle by resuspending them in fresh YPD medium containing 50 μg/ml pronase and methyl methane sulfonate (MMS) or hydroxyurea (HU). After transient MMS treatment, cells were washed with 2.5% sodium thiosulfate (a chemical that inactivates MMS) and released into fresh YPD medium. Aliquots of cells were collected as a function of time and flash frozen on dry ice before being processed for immunoblotting or pulsed-field gel electrophoresis. Where applicable, appropriate dilutions of cells were plated on YPD medium to measure viability by colony-formation assays.

Measurement of DNA content by flow cytometry

Cells were fixed with 70% ethanol prior to FACS flow cytometry analysis. DNA content was determined using Sytox Green (Invitrogen, Carlsbad, CA) as described previously (Haase and Reed 2002). Flow cytometry was performed on a Becton Dickinson LSR II instrument using the FACS Diva software (BD Biosciences, San Jose, CA) and on a FACS Calibur instrument using the Cell Quest software (BD Biosciences). Histograms were generated using FlowJo 7.6.5 (FlowJo, LLC, Ashland, OR).

Pulsed-field gel electrophoresis

Then 10^7 cells were embedded in agarose plugs and treated for pulsed-field gel electrophoresis as described previously (Maringele and Lydall 2006). Electrophoresis was performed using a Bio-Rad CHEF DRIII instrument using the manufacturer's protocols (Bio-Rad Laboratories, Hercules, CA).

Immunoblots

Whole-cell lysates were prepared for SDS-PAGE using an alkaline cell lysis (Kushnirov 2000) or standard glass bead–trichloroacetic acid precipitation methods. SDS-PAGE and protein transfers were performed using standard molecular biology protocols. Our rabbit polyclonal antibodies against H3K56Ac (AV105) and H2A phosphorylated at S128 (AV137) were described previously (Masumoto *et al.* 2005). Anti-yeast H2A was purchased from Active Motif (Cat. No 39236; Carlsbad, CA). Our rabbit polyclonal antibody (AV94) raised against recombinant yeast histone H4 expressed in *Escherichia coli* (which is devoid of H4 modifications) was described previously (Tang *et al.* 2008). Our rabbit polyclonal antibody (AV100) raised against a C-terminal peptide of H3 that is devoid of known modifications also was described previously (Gunjan and Verreault 2003). 12CA5 monoclonal antibodies were used to detect the HA epitope, and anti-Flag M2 antibodies were purchased from Sigma (St. Louis, MO). Anti-acetyl histone H4 (Lys16Ac; Cat. No 07-329) and anti-trimethylated histone H3 (Lys79Me3; ab2621) were purchased from Abcam (Cambridge, MA).

Rad53 autophosphorylation assays

Protein samples were prepared by the glass bead–tricholoroacetic acid precipitation method, resolved by SDS-PAGE, and transferred to PVDF membranes using standard Towbin buffer (25 mM Tris and 192 mM glycine) without methanol or SDS at 0.8 mA/cm^2 for 2 hr on a Bio-Rad SD semidry transfer apparatus. Membranes then were processed as described previously (Pellicioli *et al.* 1999).

Densitometry analysis

Densitometry analyses of immunoblot and Rad53 *in situ* autophosphorylation assays were performed using Image J 1.46E. Signal obtained for histone modifications were normalized

Table 1 Yeast strains used in this study

Strain	Genotype	Reference
HWY294	BY4743 *MAT**a** ura3Δ0 leu2Δ0 his3Δ1*	This study
FY833	*MAT**a** his3Δ200 leu2Δ1 lys2-202 trp1Δ63 ura3-52*	Winston *et al.* 1995
ICY703	FY833 *hst3Δ::HIS3 hst4Δ::TRP1* (p*CEN URA3 HST3*)	Celic *et al.* 2006
ICY918	FY833 *hst3Δ::HIS3 hst4Δ::TRP1* (p*CEN URA3 HST3*) *sas2Δ::kanMX*	This study
ICY1081	FY833 *hst3Δ::HIS3 hst4Δ::TRP1* (p*CEN URA3 HST3*) *rsc2Δ::kanMX*	This study
ICY1345	FY833 *hst3Δ::HIS3 hst4Δ::kanMX4 hht1-hhf1Δ:: natMX4 hht2-hhf2Δ:: hygMX4* (p*CEN URA3 HST3*) (p*CEN LYS2 HHT1-HHF1*)	This study
HWY51	FY833 *hst3Δ::HIS3 hst4Δ::kanMX hht1-hhf1::natMX hht2-hhf2::hygMX* (p*CEN TRP1 HHT2-hhf2 K16R*) (p*CEN URA3 HST3*)	This study
HWY200	FY833 *hst3Δ::HIS3 hst4Δ::TRP1* (p*CEN URA3 HST3*) *yta7Δ::LEU2*	This study
HWY186	FY833 *hst3Δ::HIS3 hst4Δ::TRP1* (p*CEN URA3 HST3*) *sir2Δ::LEU2*	This study
HWY190	FY833 *hst3Δ::HIS3 hst4Δ::TRP1* (p*CEN URA3 HST3I) sir2Δ::LEU2 sas2Δ::KanMX*	This study
HWY192	FY833 *hst3Δ::HIS3 hst4Δ::TRP1* (p*CEN URA3 HST3*) *sir2Δ::LEU2 rsc2Δ::KanMX*	This study
HWY193	FY833 *hst3Δ::HIS3 hst4Δ::KanMX hht1-hhf1::natMX hht2-hhf2::hygMX sir2Δ::LEU2* (p*CEN TRP1 HHT2-hhf2 K16R*) (p*CEN URA3 HST3*)	This study
HWY385	FY833 *hst3Δ::HIS3 hst4Δ::TRP1* (p*CEN URA3 HST3*) *cdc45::CDC45-HA::LEU2*	This study
HWY387	FY833 *hst3Δ::HIS3 hst4Δ::TRP1* (p*CEN URA3 HST3*) *sas2Δ::kanMX cdc45::CDC45-HA::LEU2*	This study
HWY406	FY833 *hst3Δ::HIS3 hst4Δ::KanMX hht1-hhf1::natMX hht2-hhf2::hygMX* (p*CEN TRP1 HHT2-hhf2 K16R*) (p*CEN URA3 HST3*) *cdc45::CDC45-HA::LEU2*	This study
Tr1	FY833 *hst3Δ::HIS3 hst4Δ::TRP1 tr1*	This study
Tr2	FY833 *hst3Δ::HIS3 hst4Δ::TRP1 tr2*	This study
Tr3	FY833 *hst3Δ::HIS3 hst4Δ::TRP1 tr3*	This study
Tr4	FY833 *hst3Δ::HIS3 hst4Δ::TRP1 tr4*	This study
Tr5	FY833 *hst3Δ::HIS3 hst4Δ::TRP1 tr5*	This study
Tr6	FY833 *hst3Δ::HIS3 hst4Δ::TRP1 tr6*	This study
Tr7	FY833 *hst3Δ::HIS3 hst4Δ::TRP1 tr7*	This study
Tr8	FY833 *hst3Δ::HIS3 hst4Δ::TRP1 tr8*	This study
Tr9	FY833 *hst3Δ::HIS3 hst4Δ::TRP1 tr9*	This study
Tr10	FY833 *hst3Δ::HIS3 hst4Δ::TRP1 tr10*	This study
Tr11	FY833 *hst3Δ::HIS3 hst4Δ::TRP1 tr11*	This study
Tr12	FY833 *hst3Δ::HIS3 hst4Δ::TRP1 tr12*	This study
DWY1	FY833 *hst3Δ::HIS3 hst4Δ::TRP1 rtt109::RTT109-Flag::His3MX6*	This study
DWY2	FY833 *hst3Δ::HIS3 hst4Δ::TRP1 rtt109::RTT109-Flag::His3MX6 tr4*	This study
DWY3	FY833 *hst3Δ::HIS3 hst4Δ::TRP1 rtt109::RTT109-Flag::His3MX6 tr6*	This study
DWY4	FY833 *hst3Δ::HIS3 hst4Δ::TRP1 rtt109::RTT109-Flag::His3MX6 tr9*	This study
DWY5	FY833 *hst3Δ::HIS3 hst4Δ::TRP1 rtt109::RTT109-Flag::His3MX6 tr11*	This study
DWY6	FY833 *hst3Δ::HIS3 hst4Δ::TRP1 rtt109::RTT109-Flag::His3MX6 tr18*	This study
ASY2368	W303 *ADE2 RAD52-YFP*	This study
ASY2369	W303 *ADE2 RAD52-YFP hst3Δ::HIS5 hst4Δ::KanMX6*	This study
HWY2493	W303 *RFA1-YFP RAD5 ADE2*	This study
ASY2391	W303 *RFA1-YFP RAD5 ADE2 hst3Δ::HIS5 hst4Δ::KanMX6*	This study
ASY2737	FY833 *hst3Δ::HIS3 hst4Δ::kanMX4 hht1-hhf1Δ:: natMX4 hht2-hhf2Δ:: hygMX4* (p*CEN URA3 HST3*) (p*CEN TRP1 HHT1-HHF1*)	This study
ASY2741	FY833 *hst3Δ::HIS3 hst4Δ::kanMX4 hht1-hhf1Δ:: natMX4 hht2-hhf2Δ:: hygMX4* (p*CEN URA3 HST3*) (p*CEN TRP1 hht1K79A-HHF1*)	This study
ASY2745	FY833 *hst3Δ::HIS3 hst4Δ::kanMX4 hht1-hhf1Δ:: natMX4 hht2-hhf2Δ:: hygMX4* (p*CEN URA3 HST3*) (p*CEN TRP1 HHT1-hhf1K16R*)	This study
ASY2749	FY833 *hst3Δ::HIS3 hst4Δ::kanMX4 hht1-hhf1Δ:: natMX4 hht2-hhf2Δ:: hygMX4* (p*CEN URA3 HST3*) (p*CEN TRP1 hht1K79R-HHF1*)	This study
ASY2755	FY833 *hst3Δ::HIS3 hst4Δ::kanMX4 hht1-hhf1Δ:: natMX4 hht2-hhf2Δ:: hygMX4* (p*CEN URA3 HST3*) (p*CEN LYS2 HHT1-HHF1*) *CDC45-3HA::LEU2*	This study
ASY2758	FY833 *hst3Δ::HIS3 hst4Δ::kanMX4 hht1-hhf1Δ:: natMX4 hht2-hhf2Δ:: hygMX4* (p*CEN URA3 HST3*) (p*CEN TRP1 hht1K79A-HHF1*) *CDC45-3HA::LEU2*	This study
ASY2761	FY833 *hst3Δ::HIS3 hst4Δ::TRP1* (*pCEN URA3 HST3*) *dot1Δ::KanMX CDC45-3HA::LEU2*	This study
HWY2550	FY833 *hst3Δ::HIS3 hst4Δ::TRP1* (*pCEN URA3 HST3*) *rad9Δ::KanMX*	This study
ASY2392	FY833 *hst3Δ::HIS3 hst4Δ::TRP1* (*pCEN-URA3-HST3*) *dot1Δ::KanMX*	This study
ASY3111	YBL574 *hht1-hhf1Δ::LEU2 hht2-hhf2Δ::HIS3* (*pCEN TRP1 HHT1-HHF1*)	Nakanishi *et al.* 2008
ASY3112	YBL574 *hht1-hhf1Δ::LEU2 hht2-hhf2Δ::HIS3* (*pCEN TRP1 hht1K79A-HHF1*)	Nakanishi *et al.* 2008
ASY3113	YBL574 *hht1-hhf1Δ::LEU2 hht2-hhf2Δ::HIS3* (*pCEN TRP1 HHT-hhf1K16A*)	Nakanishi *et al.* 2008

(continued)

Table 1, *continued*

Strain	Genotype	Reference
ASY3169	FY833 *hst3Δ::HIS3 hst4Δ::TRP1* (*pCEN-URA3-HST3*) *rev3Δ::HPHMX*	This study
ASY3171	FY833 *hst3Δ::HIS3 hst4Δ::TRP1* (*pCEN-URA3-HST3*) *dot1Δ::KanMX rev3Δ::HPHMX*	This study
ASY3176	FY833 *hst3Δ::HIS3 hst4Δ::kanMX4 hht1-hhf1Δ:: natMX4 hht2-hhf2Δ:: hygMX4* (p*CEN URA3 HST3*) (p*CEN TRP1 HHT1-hhf1K16R*)	This study
ASY3178	FY833 *hst3Δ::HIS3 hst4Δ::kanMX4 hht1-hhf1Δ:: natMX4 hht2-hhf2Δ:: hygMX4* (p*CEN URA3 HST3*) (p*CEN TRP1 hht1K79R-HHF1*)	This study

relative to the corresponding nonmodified total histone signal (*i.e.*, H4K16Ac on H4, H3K56Ac on H3, etc.). Rad53 autophosphorylation signals were normalized between samples using several bands from Ponceau S staining. To facilitate comparison between assays, normalized signal from every lane was set as a ratio of the isogenic *hst3*Δ *hst4*Δ strain for each experiment. Average band intensity was calculated using this relative ratio from at least three independent experiments.

Drug susceptibility assays

Colony-formation assays were performed as described previously (Wurtele *et al.* 2012). Colony formation was monitored after 3–5 days of incubation at the indicated temperature. Genotoxic drugs (MMS and HU) were purchased from Sigma.

Fluorescence microscopy

Cell samples were fixated using formaldehyde as described previously (Wurtele *et al.* 2012) and examined using a Zeiss AxioImager.Z2 Imager fluorescence microscope equipped with the AxioVision software. Images were analyzed using Image J 1.46E.

Automated evaluation of Rfa1-YFP foci intensity

DNA foci were assumed to be fluorescent puncta, most of them of sub-diffraction-limit size. To accurately analyze the data in a nonbiased way, an algorithm was programmed using Matlab (Mathworks, Cambridge, MA), which automatically detects puncta and computes their fluorescence intensity in images composed of several cells. The method used to detect cell and DNA foci were distinct and outlined below. Fluorescent puncta were detected using linear band-pass filters that preserved objects of a size window and suppressed noise and large structures. These filters were applied by performing two two-dimensional convolutions of the image matrix with a Gaussian and a boxcar kernel. First, the image was convolved with a Gaussian kernel of the characteristic length of the noise. Second, the image matrix was convolved with a boxcar kernel twice as big as the point-spread function. This last operation is a low-pass filter for near-diffraction-limit objects. Finally, the subtraction of the boxcar image from the Gaussian images becomes a band-pass filter to choose elements bigger than noise up to twice the diffraction limit. To limit the puncta considered in the quantifications to only those inside cells, the algorithm combined an intensity threshold and a watershed approach. The intensity threshold was established using Otsu's method. The cell fluorescence was enough to use this automatic thresholding approach to assign foreground pixels to cells and background pixels to empty space. This coarse estimation of the foreground pixels was further refined by first cleaning the mask, removing isolated objects of less than 50 pixels. Next, a morphological opening of the mask using a 4-pixel-radius disk was performed. Finally, a watershed algorithm was used to identify individual cells within the mask, and objects of size lower than 10% of the average size were removed. Only foci detected within cells were considered for statistical purposes, and plots were created, clustering the intensity of all individual foci found with all images of the same condition.

Histone purification, derivatization, and mass spectrometry

Core histones were purified from yeast strains as described previously (Guillemette *et al.* 2011), except that 10 mM nicotinamide and 30 mM sodium butyrate were added to the lysis and wash buffers. Intact core histones then were fractionated by HPLC and analyzed by mass spectrometry as described in detail in Supporting Information, File S1.

Results

Transient exposure to genotoxic drugs during S phase delays completion of DNA replication in hst3Δ hst4Δ cells

S. cerevisiae cells lacking *HST3* and *HST4* are extremely sensitive to chronic exposure to genotoxic drugs (Celic *et al.* 2006, 2008; Thaminy *et al.* 2007). Although a number of these drugs, *e.g.*, MMS and HU, interfere with DNA replication in WT cells, S phase progression and cell survival of *hst3*Δ *hst4*Δ mutants transiently exposed to MMS or HU have not been studied in detail. We first determined whether DNA damage caused by transient exposure to MMS or HU during S phase led to loss of viability of *hst3*Δ *hst4*Δ cells. Cells were synchronized in G_1 and released toward S phase in medium containing MMS, and viability before and after transient exposure to MMS was determined by counting colonies that formed on rich medium (YPD) plates lacking MMS. In contrast to WT cells, transient exposure to very low concentrations of MMS during S phase led to significant loss of viability of *hst3*Δ *hst4*Δ cells (Figure 1A, left panel). HU exposure during DNA

Table 2 Rfa1-YFP foci intensity values in *hst3Δ hst4Δ* and WT cells

			Min. after release from 0.02% MMS					
	Asyn.	**Alpha**	**0**	**60**	**120**	**180**	**240**	**360**
WT mean[a]	267	208	230	433	656	517	463	405
hst3Δ hst4Δ mean[a]	391	411	421	585	908	1152	1095	939
P-value[b]	1.3×10^{-2}	1.4×10^{-4}	5.7×10^{-31}	2.8×10^{-23}	3.7×10^{-18}	1.5×10^{-47}	2.1×10^{-38}	3.3×10^{-20}

[a] Mean intensities of systematically analyzed Rfa-YFP foci (see *Materials and Methods* for details)
[b] *P*-values were calculated using an unpaired two-tailed Student's *t*-test.

replication similarly caused loss of cell viability (Figure 1A, right panel). These results are consistent with the hypothesis that impeding DNA replication fork progression during a single S phase is sufficient to kill *hst3*Δ *hst4*Δ mutant cells.

MMS interferes with DNA synthesis by inducing 3-methyladenine, which strongly blocks the progression of replicative DNA polymerases (Beranek *et al.* 1983; Budzowska and Kanaar 2008), whereas HU acts via depletion of deoxyribonucleotide pools, thereby stalling replication fork progression (Yarbro 1992). We monitored the extent of chromosome replication in *hst3*Δ *hst4*Δ cells transiently exposed to MMS by flow cytometry (FACS) to measure DNA content and by pulsed-field gel electrophoresis (PFGE) as an indicator of chromosome integrity. Incompletely replicated chromosomes cannot migrate through pulsed-field gels, resulting in decreased intensity of intact chromosome bands stained with ethidium bromide (Maringele and Lydall 2006). After removal of MMS, WT cells completed chromosome duplication, as judged by the emergence of chromosome bands in pulsed-field gels and the fact that cells eventually completed mitosis, as demonstrated by FACS (Figure 1B, D). In striking contrast to WT cells, FACS analysis of *hst3*Δ *hst4*Δ cells indicated that DNA content increased very slowly after removal of MMS from the medium, with most cells exhibiting sub-G_2 DNA content 6 hr after MMS removal (Figure 1B). Concordant with this, none of the chromosomes entered pulsed-field gels for at least 3 hr after MMS removal from *hst3*Δ *hst4*Δ cells (Figure 1D). Similar results were obtained for *hst3*Δ *hst4*Δ cells treated with HU (Figure 1, C and E). These data indicate that replicative stress strongly delays completion of chromosome duplication in *hst3*Δ *hst4*Δ cells, which holds true for all chromosomes regardless of size.

Exposure to genotoxins causes accumulation of homologous recombination protein foci and persistent activation of DNA damage checkpoint kinases in hst3Δ hst4Δ cells

Repair of damaged DNA replication forks by homologous recombination (HR) in yeast depends on the Rad52 protein (Budzowska and Kanaar 2008; Thorpe *et al.* 2011). Importantly, in both yeast and humans, HR proteins form nuclear foci in response to certain DNA-damaging agents including MMS (Lisby *et al.* 2004; Thorpe *et al.* 2011). We hypothesized that defective replication fork recovery after DNA damage in *hst3*Δ *hst4*Δ mutant cells could engender the formation of abnormal HR structures. To test this, we generated *hst3*Δ *hst4*Δ strains expressing Rad52-YFP from its endogenous locus. Exponentially growing asynchronous *hst3*Δ *hst4*Δ cell populations presented a higher frequency of spontaneously arising Rad52-YFP foci compared with WT cells (Figure 2A).Our results also indicated that immediately after treatment with MMS during S phase, a larger fraction of *hst3*Δ *hst4*Δ cells displayed Rad52-YFP foci (up to 60%) than WT cells (Figure 2A, time 0). This behavior of *hst3*Δ *hst4*Δ mutants was unexpected because in WT cells activation of DNA damage-response (DDR) kinases has been reported to inhibit the formation of Rad52 foci during S phase, at least until MMS is removed from the medium (Alabert *et al.* 2009).

The frequency of *hst3*Δ *hst4*Δ cells containing MMS-induced Rad52-YFP foci increased progressively to reach 80% of cells at 6 hr after removal of MMS from the growth medium (Figure 2A). In contrast, the fraction of WT cells with Rad52-YFP foci peaked at 120 min after removal of MMS and then decreased. Overall, these data suggest that a DNA replication-coupled Rad52-dependent process fails to proceed normally after cells lacking Hst3 and Hst4 are transiently exposed to MMS. HR defects at sites of MMS-induced DNA lesions may cause persistent DNA strand exchange intermediates and/or regions of incompletely replicated DNA. On entry into anaphase, these aberrant structures would be expected to result in chromatin bridges between sister chromatids (Germann *et al.* 2014). We analyzed anaphase chromatin bridges by visualizing DAPI-stained cells derived from the experiment shown in Figure 2A. Compared with WT cells, a significantly larger fraction of cells devoid of Hst3 and Hst4 presented anaphase bridges after transient exposure to MMS during S phase (Figure 2B). Moreover, a large fraction of both WT and *hst3*Δ *hst4*Δ cells containing anaphase bridges was marked by Rad52-YFP foci. This suggests that at least some MMS-induced lesions may lead to incompletely replicated chromosomes and/or accumulation of HR intermediates, which, in turn, may generate mitotic anomalies and the high incidence of mitotic chromosome segregation defects observed in *hst3*Δ *hst4*Δ mutants (Brachmann *et al.* 1995; Celic *et al.* 2006).

RPA is a three-subunit single-stranded DNA binding protein complex that is essential for DNA replication in both yeast and humans (Masai *et al.* 2010). In yeast, the subunits of RPA are encoded by the *RFA1*, *RFA2*, and *RFA3* genes (Brill and Stillman 1991). RPA plays essential roles in

Table 3 Histone H3 gene mutations and phenotypes of *hst3*Δ *hst4*Δ mutant cells

Histone mutant	Sensitivity at 37°	MMS sensitivity	HU sensitivity
*hst3*Δ *hst4*Δ			
H3 WT	Ts-	S	S
H3 R2A	Ts-	S	S
H3 R2K	Ts-	S	S
H3 T6A	Ts-	S	S
H3 T6E	Ts-	S	S
H3 K9A	Ts-	S	S
H3 K9R	Ts-	S	S
H3 K9Q	Ts-	S	S
H3 S10A	Ts-	S	S
H3 S10E	Ts-	S	S
H3 T11A	Ts-	S	S
H3 T11E	Ts-	S	S
H3 K14A	Ts-	S	S
H3 K14R	Ts-	S	S
H3 K14Q	Ts-	S	S
H3 R17A	Ts-	S	S
H3 R17K	Ts-	S	S
H3 K18A	Ts-	S	S
H3 K18R	Ts-	S	S
H3 K18Q	Ts-	S	S
H3 K23A	Ts-	S	S
H3 K23R	Ts-	S	S
H3 K23Q	Ts-	S	S
H3 R26A	Ts-	S	S
H3 K26K	Ts-	S	S
H3 K27A	Ts-	S	S
H3 K27R	Ts-	S	S
H3 K27Q	Ts-	S	S
H3 WT	Ts-	S	S
H3 S28A	Ts-	S	S
H3 S28E	Ts-	S	S
H3 R52A	Ts-	S	S
H3 R52K	Ts-	S	S
H3 R52Q	Ts-	S	S
H3 R53A	Ts-	S	S
H3 R53K	Ts-	S	S
H3 R53Q	Ts-	S	S
H3 K56R	Tr	R	R
H3 K56Q	Tr	R	R
H3 K79A	Tr	R	R
H3K79R	Tr	R	R
H3 K91A	Ts-	S	S
H3 K91R	Ts-	S	S
H3 K91Q	Ts-	S	S
H3 K115A	Ts-	S	S
H3 K115R	Ts-	S	S
H3 K115Q	Ts-	S	S
H3 T118A	Ts-	S	S
H3 T118E	Ts-	S	S
H3 K122A	Ts-	S	S
H3 K122R	Ts-	S	S
H3 K122Q	Ts-	S	S

Ts-, thermosensitive (fails to grow at 37°); Tr, thermoresistant (grows at 37°); S, growth compromised on plates containing either 0.01% MMS or 100 mM HU; R, histone gene mutations that rescue, at least partially, the MMS or HU sensitivity of *hst3*Δ *hst4*Δ cells.

DNA replication, HR, and activation of DNA damage checkpoints (Krogh and Symington 2004; Branzei and Foiani 2009) and binds single-stranded DNA generated at sites of DNA lesions (Krogh and Symington 2004). As was the case for Rad52-YFP, we found that Rfa1-YFP formed persistent foci after transient exposure of *hst3*Δ *hst4*Δ mutants to MMS during S phase (Figure 2C). On visual inspection of microscopy images, we noted that Rfa1-YFP foci in *hst3*Δ *hst4*Δ cells appeared brighter than in WT cells (Figure 2D). To verify this in an unbiased manner, we developed a software program capable of analyzing the intensity of individual foci (see *Materials and Methods*). This analysis indicated that at every time point examined, Rfa1-YFP foci were significantly brighter in *hst3*Δ *hst4*Δ mutants than in WT cells, with a statistically significant increase of 1.4-fold in the absence of damage and as much as 2.2-fold 180 min after removal of MMS (Figure 2, D–E, and Table 2). This suggests that when H3K56Ac is present throughout the genome, as is the case in *hst3*Δ *hst4*Δ mutants released from G_1 toward S phase, abnormally long regions of RPA-bound single-stranded DNA may be formed at sites where DNA synthesis is impeded by MMS-induced lesions.

RPA-coated single-stranded DNA generated at blocked replication forks is critical for activation of the intra–S phase DNA damage checkpoint (Branzei and Foiani 2009). Current models propose that the apical DDR kinase Mec1 is activated at sites of DNA lesions through its interaction with the Ddc2 adapter protein, which binds to RPA-coated single-stranded DNA (Zou and Elledge 2003). Extensive single-stranded DNA regions formed at damaged DNA replication forks in *hst3*Δ *hst4*Δ mutants exposed to MMS should lead to robust DDR kinase activity. Phosphorylation of *S. cerevisiae* histone H2A on serine 128 (H2AP), the functional counterpart of H2AX serine 139 phosphorylation (γ-H2AX) in vertebrates, is a well-established marker of DNA damage. H2AP formation is catalyzed by the DDR kinases Mec1 and Tel1 (Downs *et al.* 2000). After transient exposure to MMS, both WT and *hst3*Δ *hst4*Δ cells showed increased H2AP (Figure 3A). In WT cells, the H2AP signal declined as a function of time after removal of MMS, suggesting progressive repair of DNA damage as well as inactivation of Mec1/Tel1 (Figure 3A). In contrast, H2AP levels remained high in *hst3*Δ *hst4*Δ cells for at least 4.5 hr after removal of MMS (Figure 3A). The persistence of high levels of H2AP in *hst3*Δ *hst4*Δ cells transiently exposed to MMS during S phase is consistent with robust and long-lasting DDR kinase activity in response to unrepaired DNA lesions. We assessed the activity of Rad53, a DDR kinase that is phosphorylated and activated by Mec1 following DNA damage (Pellicioli *et al.* 1999; Sweeney *et al.* 2005). As measured by *in situ* autophosphorylation assays, the kinase activity of Rad53 was inactivated after MMS removal from the medium in WT cells (Figure 3B). In contrast, Rad53 activity remained elevated for at least 4.5 hr in *hst3*Δ *hst4*Δ mutants (Figure 3B). This indicates that in contrast to WT cells, DDR kinases remain active for long periods after transient exposure of *hst3*Δ *hst4*Δ cells to genotoxic agents. We further note that activated Rad53 and phosphorylated H2A are detectable in asynchronous *hst3*Δ *hst4*Δ cells even in the absence of genotoxic stress

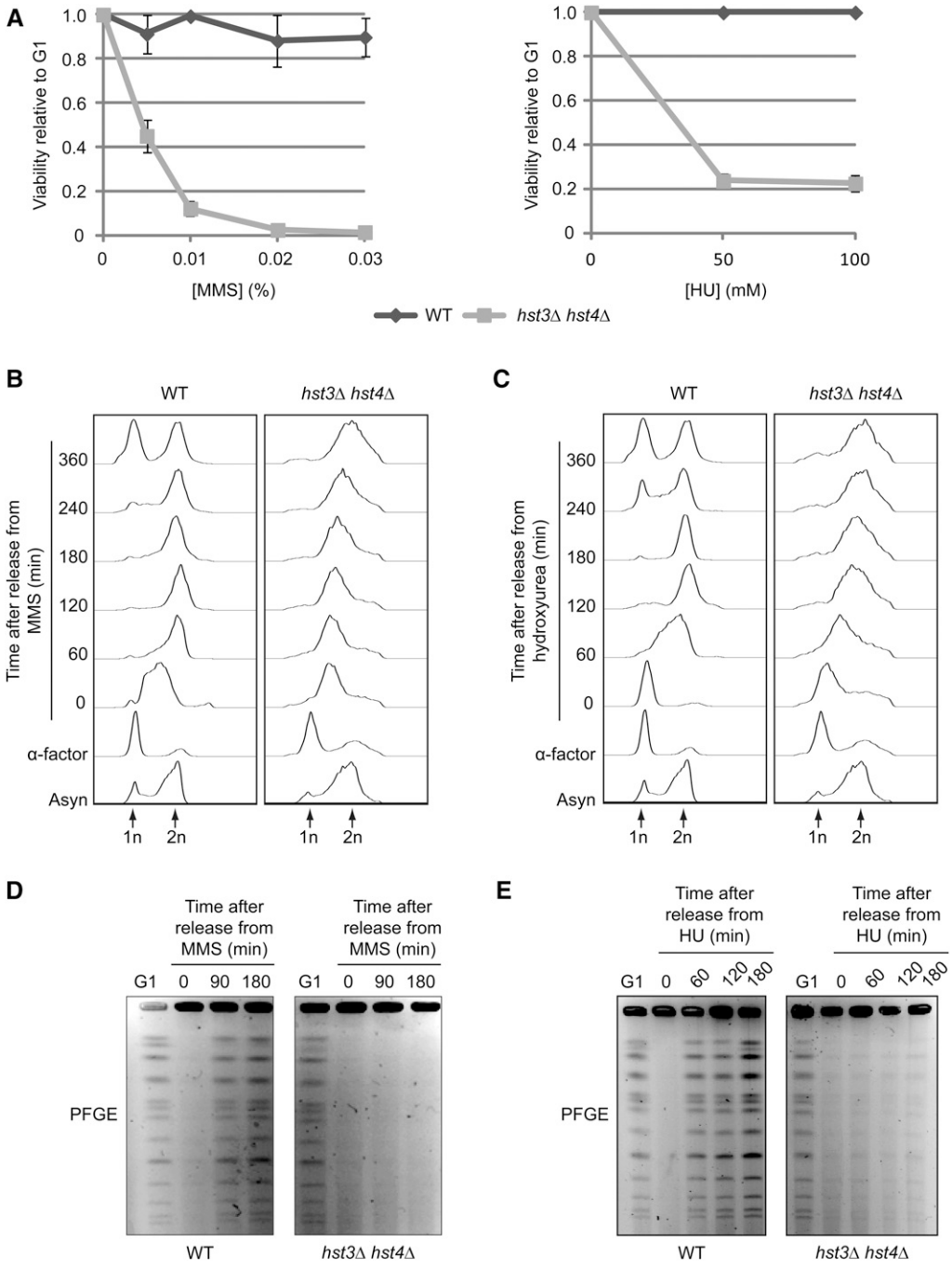

Figure 1 Transient exposure of *hst3*Δ *hst4*Δ cells to MMS or HU causes loss of viability and prevents the completion of DNA replication. (A) *hst3*Δ *hst4*Δ cells are sensitive to transient exposure to MMS and HU during S phase. Cells were arrested in G_1 and released into the cell cycle in the presence of increasing concentrations of MMS (left panel) or HU (right panel) at 25°. Appropriate dilutions of cells were plated on YPD during G_1 arrest and after 90 min of MMS exposure. Viability was defined as the ratio of colonies that arose after MMS or HU treatment to colonies formed by G_1-synchronized cells (see *Materials and Methods*). (B and C) Transient exposure to MMS or HU delays the completion of DNA replication in *hst3*Δ *hst4*Δ mutants. Cells were synchronized in G_1 with α-factor and released toward S phase in a medium containing 0.03% MMS or 200 mM HU for 90 min. Genotoxic agents then were washed away and inactivated using 2.5% sodium thiosulfate in the case of MMS, and cells were released into fresh medium lacking genotoxins. Samples were processed for cell-cycle analysis by FACS at the indicated time points. Asyn, asynchronous cells. (D and E) *hst3*Δ *hst4*Δ mutants cannot complete chromosome duplication after transient exposure to MMS. Cells were arrested in G_1 and released into the cell cycle in the presence of 0.03% MMS or 200 mM HU for 1.5 hr. They were washed with YPD (containing 2.5% sodium thiosulfate in the case of MMS) and resuspended in fresh medium lacking genotoxins. Samples were taken at the indicated time points and processed for pulse-field gel electrophoresis.

(Figure 6, B and C), indicating constitutive activation of DDR kinases in these mutants. Overall, our results indicate that cells lacking Hst3 and Hst4 manifest persistent DNA damage–induced signaling in response to MMS-induced DNA lesions.

Previously published results suggested that cells lacking Hst3 and Hst4 may present defects in activation of the intra–S phase branch of the DNA damage checkpoint (Thaminy *et al.* 2007). Mrc1 is an important component of the intra–S phase checkpoint that promotes rapid activation of Rad53 in response to HU (Alcasabas *et al.* 2001; Osborn and Elledge 2003). Rad9 is partially redundant with Mrc1 in this regard, and because of this, *mrc1*Δ *rad9*Δ cells are defective in Rad53 activation after exposure to HU. Deletion of *MRC1* also permits formation of Rad52 foci during MMS exposure, which form only after MMS has been removed from the growth medium in WT cells (Alabert *et al.* 2009). The HU sensitivity (Figure 1A) and abnormal formation of Rad52 foci during MMS exposure (Figure 2A) observed in *hst3*Δ *hst4*Δ mutants are consistent with defects in intra–S phase

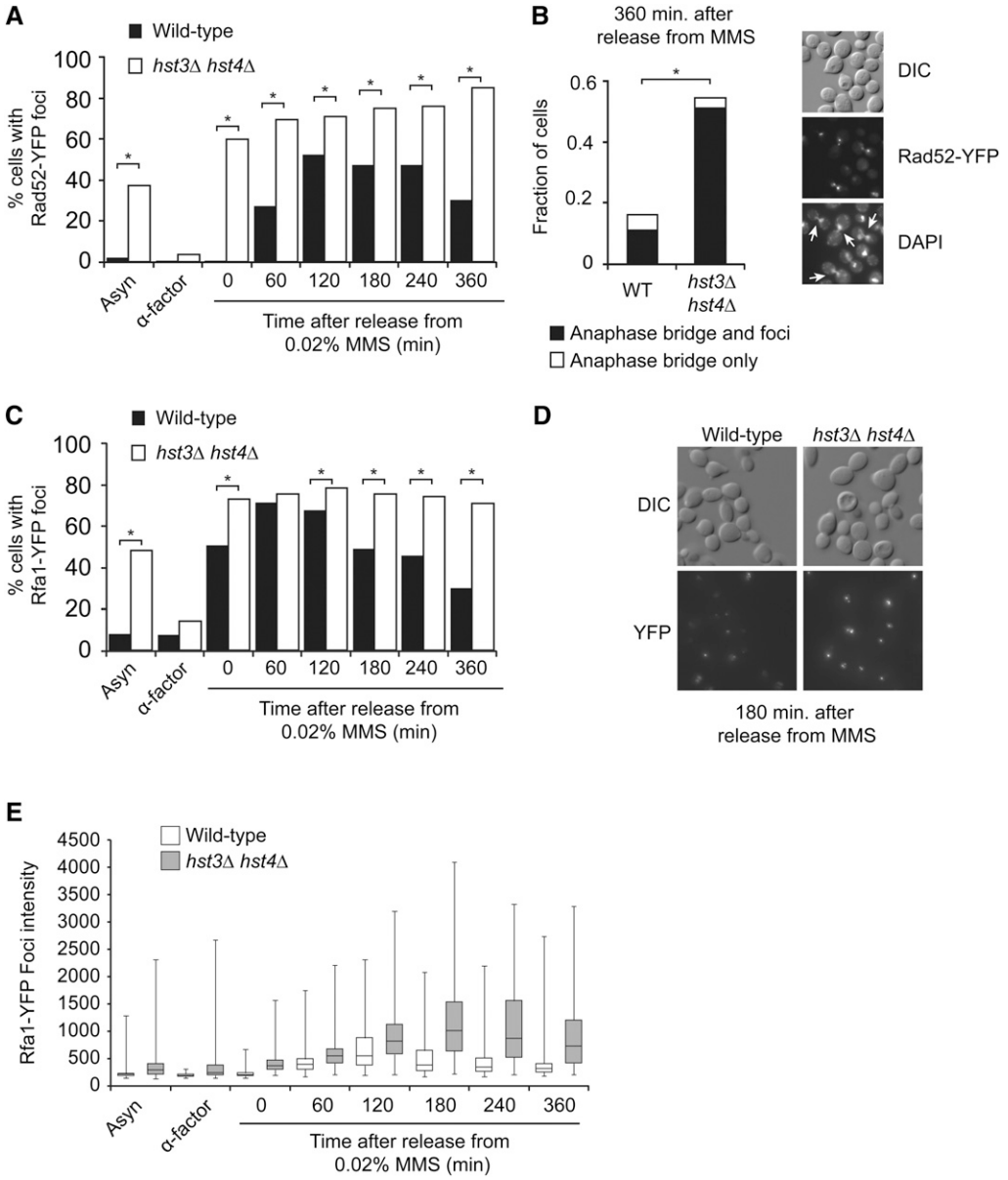

Figure 2 *hst3*Δ *hst4*Δ cells present abnormal frequencies of spontaneous and MMS-induced Rad52 and Rfa1 foci. (A) Formation of persistent Rad52-YFP foci in *hst3*Δ *hst4*Δ mutants transiently exposed to MMS during S phase. Cells were synchronized in G_1 and released toward S phase in the presence of 0.02% MMS for 90 min at 25°. MMS was inactivated using sodium thiosulfate–containing medium, and cells were incubated in fresh medium without MMS. Samples were taken at the indicated time points, and Rad52-YFP foci were detected by fluorescence microscopy. At least 300 cells were analyzed for each time point; results from a representative experiment are shown. **P*-value < 0.0001; χ^2 test. (B) *hst3*Δ *hst4*Δ mutants display anaphase bridges after transient exposure to MMS during S phase. Images of DAPI staining and Rad52-YFP foci from the "360 min" sample in A were analyzed for the presence of anaphase bridges. (Left panel) Fraction of cells containing anaphase bridge with or without Rad52-YFP foci. (Right panel) Representative image of anaphase bridges (indicated by arrows). More than 350 cells were analyzed. **P*-value $<$ 0.0001; χ^2 test. (C and D) Transient MMS exposure during S phase causes the formation of persistent Rfa1-YFP foci in *hst3*Δ *hst4*Δ mutants. (C) Cells were treated as in A, except that samples were analyzed for the presence of Rfa1-YFP foci by fluorescence microscopy. A representative experiment is shown. More than 300 cells were analyzed for each time point. **P*-value < 0.0001; Fisher's exact test. (D) Representative images of the "180 min" time point from C. (E) The intensity of Rfa1-YFP foci was analyzed using a custom-made software (see *Materials and Methods* for details). Whiskers of the box-and-whiskers plot represent the first and fourth quartiles of the distribution. Statistical analysis of these data are presented in Table 2.

checkpoint activity. We sought to determine whether Rad53 activation was indeed defective in response to HU in *hst3*Δ *hst4*Δ cells. Our *in situ* autophosphorylation assays indicate that Rad53 activation after HU treatment is comparable or perhaps even slightly higher in *hst3*Δ *hst4*Δ mutants than in WT cells (Figure 3C). In addition, we did not observe a significant reduction in Rad53 autophosphorylation in *hst3*Δ *hst4*Δ *rad9*Δ triple mutants relative to *hst3*Δ *hst4*Δ cells after exposure to HU, indicating that the Mrc1 branch of the intra–S phase DNA damage checkpoint is most likely active in these mutants (Figure 3C). Overall, our results suggest that the HU sensitivity of *hst3*Δ *hst4*Δ cells (Figure 1A) or the untimely formation of Rad52 foci when this mutant is treated with MMS (Figure 2A) cannot be accounted for by complete loss of function of the intra–S phase branch of the DNA damage checkpoint.

*Mutations that perturb chromatin structure suppress hst3*Δ *hst4*Δ *phenotypes*

The phenotypes of *hst3*Δ *hst4*Δ mutants appear to depend on the fact that unlike in WT cells, the vast majority of H3 molecules are K56 acetylated and/or that H3K56 hyperacetylation is present continuously throughout the cell cycle. Consistent with this, an *H3K56R* mutation that abolishes H3K56Ac suppresses many of these phenotypes (Celic *et al.* 2006, 2008; Miller *et al.* 2006). We sought to determine whether other histone gene mutations suppress the temperature and/or genotoxic agent sensitivity of *hst3*Δ

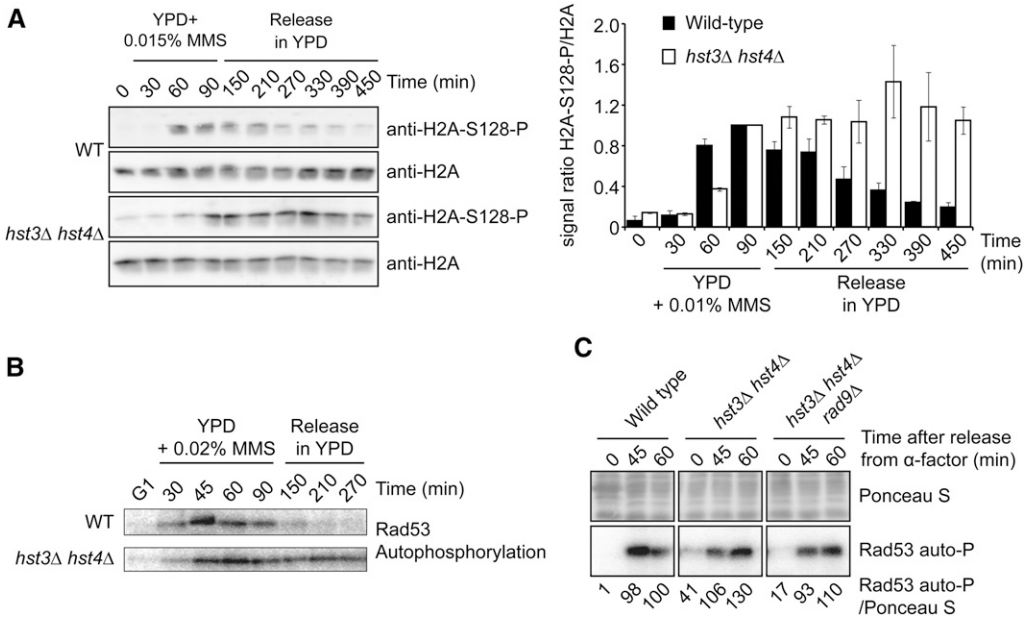

Figure 3 Persistent activation of DNA damage–induced signaling in *hst3*Δ *hst4*Δ mutants exposed to MMS. (A) *hst3*Δ *hst4*Δ mutants display persistent phosphorylation of histone H2A serine 128 following transient exposure to MMS. Cells were arrested in G_1 and released into the cell cycle in the presence of 0.015% MMS for up to 90 min. Cells were washed in YPD medium containing 2.5% sodium thiosulfate to inactivate MMS and resuspended in fresh YPD without MMS. (Left panel) Aliquots of cells were collected, and whole-cell lysates were analyzed by immunoblotting to detect histone H2A S128 phosphorylation (H2A-S128-P) and nonmodified H2A. (Right panel) H2A-S128-P signals were quantified by densitometry and normalized relative to H2A levels. For both strains, the value of time point "90 min" (end of MMS exposure) was set to 1, and values for other samples were normalized relative to this point. Error bars: standard error of the mean of densitometry values (three loadings of the immunoblot samples). (B) Cells were treated as in A except that 0.02% MMS was used, and autophosphorylation of Rad53 was detected using *in situ* kinase assay (see *Materials and Methods*). (C) *hst3*Δ *hst4*Δ *rad9*Δ triple mutants do not display Rad53 activation defects in response to HU-induced replication block. Cells were synchronized in G_1 using α-factor and released into YPD medium containing 200 mM HU. Samples were taken at the indicated time points, and Rad53 activity was monitored by *in situ* Rad53 autophosphorylation assay (Rad53 auto-P). Equal amounts of total protein were loaded for each sample. Rad53 autophosphorylation signals were quantified by densitometry relative to Ponceau S staining. Values were normalized to the "60 min" sample of the WT strain.

*hst4*Δ cells by screening a collection of histone H3/H4 mutants (Hyland *et al.* 2005). To this end, we generated *hst3*Δ *hst4* strains expressing histone point mutants from a low-copy centromeric *TRP1* plasmid. These strains also harbored a p*CEN-URA3-HST3* plasmid to prevent the emergence of spontaneous suppressors that arise during long-term propagation of *hst3*Δ *hst4*Δ mutants (see *Materials and Methods*). To test their genotoxic drug and temperature sensitivity, cells were grown on medium containing 5-FOA and genotoxins at different temperatures to select against the p*CEN-URA3-HST3* plasmid (Celic *et al.* 2006). As expected, we found that mutations at H3K56 partially suppressed the temperature, HU, and MMS sensitivity of *hst3*Δ *hst4*Δ mutants (Table 3), thus validating the conditions under which the screen was conducted. We note that this suppression is only partial because the triple mutants *hst3*Δ *hst4*Δ *H3K56R* retain the genotoxic agent sensitivity of cells lacking H3K56Ac (Celic *et al.* 2006).

Most H3/H4 point mutations, including those involving basic residues near H3K56 (H3R52 and R53), did not noticeably modulate *hst3*Δ *hst4*Δ phenotypes (Table 3 and Table 4). We also found that certain mutations of H4K20 (H4K20A or Q) slightly rescued the Ts- phenotype (Table 4 and data not shown). In contrast, mutation of histone H4 lysine 16 and H3 lysine 79 to either arginine or alanine strongly suppressed temperature sensitivity, as well as sensitivity to either chronic or transient MMS exposure (Table 3, Table 4, and Figure 4, A–C). Densitometry analyses of immunoblots indicated that the *H4K16R* and *H3K79R* mutations did not reduce H3K56Ac levels (Figure 4D and Figure S1A). We confirmed these results in a more precise manner using quantitative mass spectrometry (File S1 and Table 5), which revealed that the stoichiometry of H3K56Ac was indeed not reduced in *hst3*Δ *hst4*Δ cells harboring either *H4K16R* or *H3K79R* mutations compared with *hst3*Δ *hst4*Δ mutants. Overall, the results of our screen suggest a previously unreported interplay among H3K56, H3K79, and H4K16 in the DNA damage response.

H4K16 acetylation (H4K16Ac) and H3K79 methylation (H3K79Me) are very abundant histone modifications in both yeast and humans (Smith *et al.* 2002; Nguyen and Zhang 2011). We evaluated whether H4K16Ac and H3K79Me contribute to the severe phenotypes of *hst3*Δ *hst4*Δ cells. In *S. cerevisiae*, the SAS-I acetyltransferase complex (composed of Sas2, Sas4, and Sas5) is primarily responsible for histone H4 lysine 16 acetylation (Kimura *et al.* 2002; Suka *et al.* 2002; Sutton *et al.* 2003). We found that deletion of *SAS2*, which encodes the catalytic subunit of the SAS-I complex (Sutton *et al.* 2003), resulted in partial suppression of the temperature and MMS sensitivity of *hst3*Δ *hst4*Δ mutants (Figure 4, A–C). The degree of suppression imparted by *sas2*Δ was not as pronounced as that conferred by an *H4K16R* mutation, possibly reflecting the fact that H4K16Ac is completely abolished in *H4K16R* mutants, but detectable amounts of H4K16Ac persist in *sas2*Δ cells (Figure 4D). We cannot exclude that in addition to abolishing H4K16Ac, mutation of H4K16 to either arginine or alanine also may in itself contribute to the phenotypic suppression of *hst3*Δ *hst4*Δ cells.

Table 4 Histone H4 gene mutations and phenotypes of *hst3*Δ *hst4*Δ mutant cells

Histone mutant	Sensitivity at 37°	MMS sensitivity	HU sensitivity
*hst3*Δ *hst4*Δ			
H4 WT	Ts-	S	S
H4 S1A	Ts-	S	S
H4 S1E	Ts-	S	S
H4 R3A	Ts-	S	S
H4 R3K	Ts-	S	S
H4 K5A	Ts-	S	S
H4 K5R	Ts-	S	S
H4 K5Q	Ts-	S	S
H4 K8A	Ts-	S	S
H4 K8R	Ts-	S	S
H4 K8Q	Ts-	S	S
H4 K12A	Ts-	S	S
H4 K12R	Ts-	S	S
H4 K12Q	Ts-	S	S
H4 K16R	Tr	R	S
H4 K16A	Tr	R	S
H4 K20A	Tr	R	S
H4 K20R	Ts-	S	S
H4 K20Q	Tr	R	S
H4 K31A	Ts-	S	S
H4 K31R	Ts-	S	S
H4 K31Q	Ts-	S	S
H4 S47A	Ts-	S	S
H4 S47E	Ts-	S	S
H4 K59A	Ts-	S	S
H4 K59R	Ts-	S	S
H4 K59Q	Ts-	S	S
H4 K77A	Ts-	S	S
H4 K77R	Ts-	S	S
H4 K77Q	Ts-	S	S
H4 K79A	Ts-	S	S
H4 K79R	Ts-	S	S
H4 K79Q	Ts-	S	S
H4 K91A	Ts-	S	S
H4 R91R	Ts-	S	S
H4 K91Q	Ts-	S	S
H4 R92A	Ts-	S	S
H4 R92K	Ts-	S	S

Ts-, thermosensitive (fails to grow at 37°); Tr, thermoresistant (grows at 37°); S, growth compromised on plates containing either 0.01% MMS or 100 mM HU; R, histone gene mutations that rescue, at least partially, the MMS or HU sensitivity of *hst3*Δ *hst4*Δ cells.

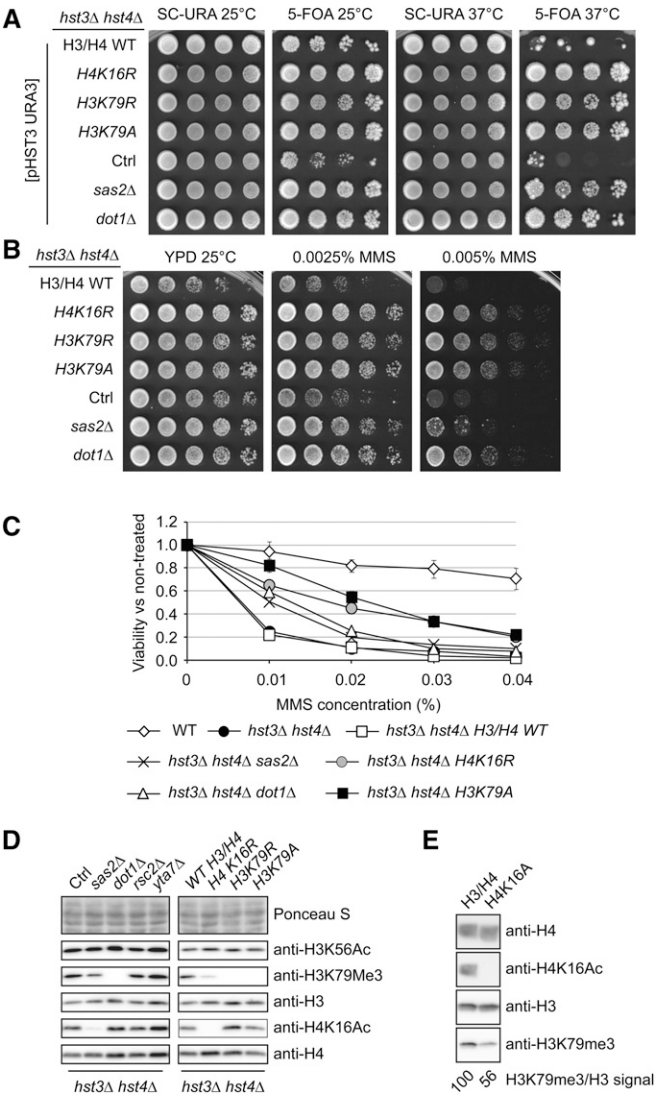

Figure 4 Mutations that prevent modifications of H3 lysine 79 or H4 lysine 16 suppress the MMS sensitivity and Ts- phenotypes of *hst3*Δ *hst4*Δ mutants. (A) Mutations of enzymes that methylate H3K79 or acetylate H4K16, or point mutations of these residues, suppress the Ts- phenotype of *hst3*Δ *hst4*Δ mutants. Fivefold serial dilutions of cells carrying a centromeric plasmid expressing *URA3* and *HST3* were spotted on the indicated medium and grown at either 25 or 37°. (B and C) The sensitivity of *hst3*Δ *hst4*Δ mutants to MMS is rescued by mutations that reduce H3K79 methylation or H4K16Ac. (B) Fivefold serial dilutions of cells were spotted onto YPD medium containing MMS and incubated at 25°. (C) Exponentially growing cells were exposed to increasing concentrations of MMS for 90 min at 25°. Viability was defined as the ratio of the number of colonies that arose after MMS treatment to the number colonies formed by cells that were not exposed to MMS. Error bars, standard error of the mean from at least three independent experiments for each strain. (D and E) Whole-cell lysates of exponentially growing cells were probed by immunoblotting using the indicated antibodies (see Figure S1 for densitometry analysis). Ctrl, *hst3*Δ *hst4*Δ cells.

The methyltransferase Dot1 is responsible for H3K79 mono-, di-, and trimethylation in yeast (van Leeuwen *et al.* 2002; Smith *et al.* 2002). We found that deletion of *DOT1* in *hst3*Δ *hst4*Δ cells strongly suppressed their temperature and MMS sensitivity (Figure 4, A–C). Importantly, deletion of either *DOT1* or *SAS2* did not reduce the level of H3K56Ac (Figure 4D and Figure S1A), indicating that both H3K79 methylation and H4K16 acetylation contribute to the phenotypes of *hst3*Δ *hst4*Δ cells via other mechanisms.

We did not detect elevated levels of H3K79 trimethylation or H4K16 acetylation when *hst3*Δ *hst4*Δ mutants were compared with WT cells (data not shown). However, densitometry analyses of immunoblots revealed a reproducible, albeit modest, reduction in H3K79 trimethylation levels in *hst3*Δ *hst4*Δ *sas2*Δ and *hst3*Δ *hst4*Δ *H4K16R* cells (Figure 4D and Figure S1C). This result was unexpected because previous publications examining the relationship between H4K16 acetylation and H3K79 trimethylation did not report

Table 5 Calculated relative abundance (percent of total histone H3) for H3 K79 methylation and H3 K56ac[a]

	Yeast genetic background[b]		
	*hst3*Δ *hst4*Δ H3/H4 WT (ASY2737)	*hst3*Δ *hst4*Δ H3/H4K16R (ASY2745)	*hst3*Δ *hst4*Δ H3K79R/H4 (ASY2749)
H3K79Me0 ± SEM[c,d]	13.1 ± 0.4	10 ± 1	NA
H3K79Me1 ± SEM[c,d]	4.9 ± 0.1	8 ± 1	NA
H3K79Me2 ± SEM[c,d]	11.6 ± 0.4	26 ± 2	NA
H3K79Me3 ± SEM[c,d]	70.4 ± 0.1	56 ± 4	NA
H3K56Ac ± SEM[c,e]	80.3 ± 0.7	92.4 ± 0,5	88.3 ± 0.3

NA, not applicable.

[a] The abundance of each peptide was assessed by mass spectrometry of total histone H3 purified from each strain in buffers containing a cocktail of deacetylase inhibitors (see *Materials and Methods*).

[b] Strains ASY2737, ASY2745, and ASY2749 are in the same genetic background (see Table 1).

[c] Standard error of the mean of two mass spectrometry technical replicates.

[d] The values for the different forms of H3K79 reflect the relative abundance of a given isoform (*e.g.*, H3K79me0) expressed as a percentage of the abundance of all H3K79 isoforms (K79me0+me1+me2+me3). For technical reasons, these values should not be equated stoichiometries. See *Materials and Methods* for a more detailed explanation.

[e] The values for H3K56Ac reflect stoichiometries, *i.e.*, the fraction of all H3 molecules that are K56 acetylated. This is expressed as percentages obtained as follows: abundance of K56Ac divided by abundance of K56Ac + K56Pr. See *Materials and Methods* for a more detailed explanation.

reduced H3K79 trimethylation in cells where H4K16 cannot be acetylated (Fingerman *et al.* 2007; Evans *et al.* 2008). Interestingly, we obtained similar immunoblotting results (*i.e.*, reduced H3K79 trimethylation) in *HST3 HST4* cells expressing *H4K16A*, suggesting that this effect is not restricted to cells that present abnormally high levels of H3K56Ac (Figure 4E and Figure S1D). To validate these results, we evaluated the relative abundance of mono-, di-, and trimethylated histone H3K79 using quantitative mass spectrometry (Table 5). The data indicate a modest reduction in H3K79 trimethylation in *hst3*Δ *hst4*Δ *H4K16R* cells compared with isogenic *hst3*Δ *hst4*Δ H3/H4 WT cells (compare strain ASY2737 with ASY2745 in Table 5). Consistent with such a decrease in H3K79 trimethylation, levels of both mono- and dimethylated H3K79 in *hst3*Δ *hst4*Δ *H4K16R* mutants were increased in comparison with those observed in *hst3*Δ *hst4*Δ H3/H4 WT cells. For example, the ratio of tri- to dimethylation of H3K79 is approximately three times higher in *hst3*Δ *hst4*Δ H3/H4 WT cells than in *hst3*Δ *hst4*Δ *H4K16R* cells (ratios of 6.1 *vs.* 2.2, respectively). This is consistent with immunoblotting data from Evans *et al.* (2008), who reported increased levels of H3K79 mono- and dimethylation in yeast strains harboring the *H4K16R* mutation. Overall, our data indicate that H4K16 acetylation and H3K79 methylation both contribute to the severe phenotypes caused by H3K56 hyperacetylation and raise the intriguing possibility that suppression of *hst3*Δ *hst4*Δ mutant phenotypes by the *H4K16R* mutation may be, at least in part, due to a decrease in H3K79 trimethylation.

H4K16Ac and H3K79Me are involved in preventing heterochromatin from invading euchromatic regions (Kimura *et al.* 2002; Smith *et al.* 2002; Suka *et al.* 2002; van Leeuwen *et al.* 2002; Jambunathan *et al.* 2005; Raisner and Madhani 2008). Hence, we tested whether suppression of *hst3*Δ *hst4*Δ phenotypes resulting from decreased H4K16Ac or H3K79Me might also be observed in other mutants in which chromatin boundary functions are impaired. Rsc2 is a subunit of one of the two forms of the ATP-dependent chromatin structure remodeling (RSC) complex (Cairns *et al.* 1999; Clapier and Cairns 2009). The RSC complex facilitates a number of cellular functions (Cairns *et al.* 1999; Floer *et al.* 2010; Chambers *et al.* 2012) but is critical for restricting the spread of silencing factors from heterochromatin into euchromatin (Jambunathan *et al.* 2005). Likewise, Yta7 contributes to the function of chromatin boundaries (Jambunathan *et al.* 2005; Tackett *et al.* 2005; Raisner and Madhani 2008). We found that deletion of either *RSC2* or *YTA7* partially suppressed the phenotypes of *hst3*Δ *hst4*Δ cells, although to a lesser extent than *H4K16R* or *H3K79R* mutations (Figure 5, A and C). H4K16Ac, H3K79Me3, and H3K56Ac levels were not affected in mutants lacking either Rsc2 or Yta7 (Figure 4D and Figure S1, A–C), indicating that *rsc2*Δ and *yta7*Δ mutations do not suppress the phenotypes of *hst3*Δ *hst4*Δ cells by influencing these histone modifications. We also found that deletion of *RSC1*, which forms an alternative RSC complex playing a less important role in restricting the spread of silencing in yeast (Jambunathan *et al.* 2005), causes synthetic growth defect in combination with *hst3*Δ *hst4*Δ mutations (Figure 5B). Overall, these results support a model in which modulation of chromatin boundary function may partly account for the suppressor effect of H3K79 and H4K16 mutations on *hst3*Δ *hst4*Δ phenotypes.

Sir2 deacetylates both H3K56 and H4K16 *in vitro* (Imai *et al.* 2000; Tanny and Moazed 2001; Xu *et al.* 2007). *In vivo*, the importance of Sir2 for H4K16 deacetylation in heterochromatic regions is undisputed (Kimura *et al.* 2002; Suka *et al.* 2002), but whether Sir2 plays a role in H3K56 deacetylation within heterochromatic domains is controversial (Xu *et al.* 2007; Yang *et al.* 2008). Indeed, there is substantial evidence that even within heterochromatic domains, Hst3 and Hst4 are needed for deacetylation of H3K56, while Sir2 is not (Yang *et al.* 2008). Despite the aforementioned controversy, one model to explain how perturbation of chromatin boundaries suppresses *hst3*Δ *hst4*Δ phenotypes would be that when boundaries are defective, Sir2 might spread from heterochromatic domains and remove H3K56Ac and/or

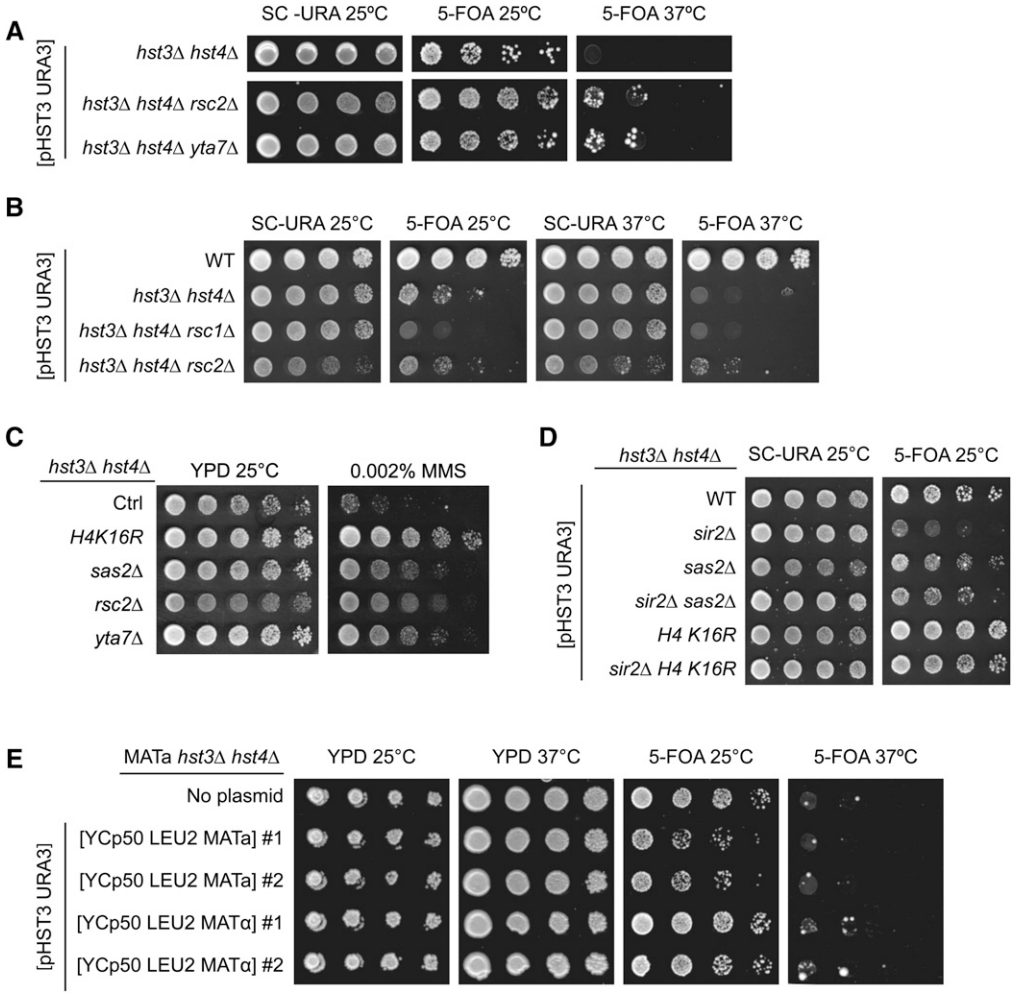

Figure 5 Mutation of genes involved in maintaining euchromatin-heterochromatin boundaries suppresses the phenotypes of *hst3*Δ *hst4*Δ mutants. (A and B) Mutations of *YTA7* or *RSC2* but not *RSC1* partially suppress the temperature sensitivity of *hst3*Δ *hst4*Δ mutants. Fivefold serial dilutions of cells carrying a centromeric plasmid expressing *URA3* and *HST3* were spotted on the indicated medium and grown at either 25 or 37°. (C) The sensitivity of *hst3*Δ *hst4*Δ mutants to MMS is partially rescued by *rsc2*Δ or *yta7*Δ mutations. Fivefold serial dilutions of cells were spotted onto YPD medium lacking or containing MMS and incubated at 25°. (D) The suppressor effect of *sas2*Δ and *H4K16R* mutations on the temperature sensitivity of *hst3*Δ *hst4*Δ cells does not require *SIR2*. Cells were treated as in A. (E) Constitutive expression of silent mating loci genes does not suppress the temperature sensitivity of *hst3*Δ *hst4*Δ cells. *MAT***a** *hst3*Δ *hst4*Δ cells harboring plasmids expressing either *MAT***a** or *MATα* genes and a centromeric plasmid expressing *URA3* and *HST3* were spotted on the indicated medium and grown at either 25 or 37°.

H4K16Ac within euchromatin, leading to partial phenotypic suppression. This model predicts that Sir2 should be essential for the suppressor effect of *H4K16R* or *sas2*Δ mutations on the phenotypes of cells lacking Hst3 and Hst4. Our results and those of Brachmann *et al.* (1995) show that a *sir2*Δ mutation exacerbates the phenotypes of *hst3*Δ *hst4*Δ cells (Figure 5D). Interestingly, we found that the *sas2*Δ and *H4K16R* mutations suppress the growth defects of *hst3*Δ *hst4*Δ *sir2*Δ cells (Figure 5D), which strongly argues that the suppression of *hst3*Δ *hst4*Δ mutant phenotypes caused by *SAS2* deletion or H4K16 mutations does not depend on deregulated Sir2-mediated histone deacetylation.

Sas2, Rsc2, and Yta7 are involved in the maintenance of chromatin boundaries at the silent mating loci (Jambunathan *et al.* 2005; Tackett *et al.* 2005; Raisner and Madhani 2008). Heterochromatin spreading in *sas2*Δ, *rsc2*Δ, or *yta7*Δ mutants likely requires that limiting pools of Sir complexes spread beyond their normal domains of action (Smith *et al.* 1998; Hoppe *et al.* 2002). Indeed, dilution of Sir2 over larger genomic domains has been proposed to reduce the efficacy of silencing in *sas2*Δ, *rsc2*Δ, or *yta7*Δ mutants. Because of this, these mutants may abnormally express the *HMR***a** and/or *HMLα* genes located at silent loci, thus generating pseudo-diploid cells (haploid cells that express genes from both mating types), which are more resistant than haploid *MAT***a** or *MATα* cells to genotoxic agents such as MMS (Livi and Mackay 1980; Barbour and Xiao 2006). To test whether abnormal gene expression derived from *HMLα* and *HMR***a** contributes to the suppression of *hst3*Δ *hst4*Δ mutant phenotypes, we transformed *hst3*Δ *hst4*Δ *MAT***a** cells with plasmids expressing either the *MAT***a** or *MATα* mating cassettes (Figure 5E). These plasmids have been reported to suppress the MMS sensitivity of several DNA repair mutants of the opposite mating type (Barbour and Xiao 2006). Our results revealed that ectopic expression of *MATα* mating-type genes did not rescue the temperature sensitivity of *hst3*Δ *hst4*Δ *MAT***a** cells (Figure 5E), which indicates that rendering *hst3*Δ *hst4*Δ mutants pseudodiploid is not sufficient to suppress their phenotypes. In turn, these data suggest that suppression of *hst3*Δ *hst4*Δ mutant phenotypes by deletion of *SAS2*, *RSC2*, or *YTA7* is unlikely to be explained by pseudodiploidy. However, we cannot exclude the possibility that abnormal gene expression resulting from disruption of chromatin boundaries could contribute to the suppression of *hst3*Δ *hst4*Δ mutant phenotypes by deletion of *RSC2* and *YTA7* and mutations of H4K16 or H3K79.

DDR kinase activity contributes to the severe phenotypes of hst3Δ hst4Δ cells

Rad9 is an adaptor protein that permits Mec1-mediated phosphorylation and activation of Rad53 in response to DNA damage (Pellicioli and Foiani 2005; Sweeney *et al.* 2005). Rad9 was previously shown to be important for the constitutive activation of Rad53 observed in *hst3*Δ *hst4*Δ mutants (Celic *et al.* 2008). Rad9 binds methylated H3K79 via its Tudor domain, thereby promoting its recruitment to chromatin, where it mediates Rad53 activation (Wysocki *et al.* 2005; Javaheri *et al.* 2006; Toh *et al.* 2006; Grenon *et al.* 2007). We hypothesized that a decrease in H3K79Me would impair Rad9 binding to chromatin and, consequently, reduce Rad53 activity to alleviate some of the phenotypes that result from H3K56 hyperacetylation. Consistent with this hypothesis, we found that deletion of *RAD9* partially suppressed the phenotypes of *hst3*Δ *hst4*Δ cells (Figure 6A) and that mutations of *DOT1*, *SAS2*, H4K16, or H3K79 noticeably decreased spontaneous and MMS-induced Rad53 activation (Figure 6, B and C, and Figure S2, A, C, and D). Interestingly, none of the suppressor mutations that we identified significantly modulated spontaneous Mec1/Tel1-mediated histone H2A phosphorylation, suggesting that these mutations may preferentially affect Rad53 activity (Figure 6B and Figure S2B).

Previously published data indicate that cells lacking Dot1 are more resistant to MMS-induced DNA damage than WT cells, and this increased resistance to MMS has been correlated with reduced levels of Rad53 activation (Conde and San-Segundo 2008; Conde *et al.* 2010; Lévesque *et al.* 2010). The sensitivity to MMS of certain yeast mutants (including *rad52*Δ and *rtt107*Δ*)* is also reduced in the absence of Dot1 or H3K79 trimethylation (Conde and San-Segundo 2008; Conde *et al.* 2010; Lévesque *et al.* 2010). We sought to verify whether the sensitivity to MMS of mutants of the H3K56Ac pathway also was suppressed by *DOT1* mutations. We deleted *DOT1* in *rtt109*Δ and *ctf4*Δ strains, which are known to be extremely sensitive to MMS (Kouprina *et al.* 1992; Han *et al.* 2007a; Celic *et al.* 2008; Wurtele *et al.* 2012). Importantly, *RTT109* and *CTF4* display extensive genetic and biochemical links to H3K56Ac and *HST3/HST4* (Collins *et al.* 2007; Han *et al.* 2007a, p. 109; Celic *et al.* 2008). In contrast to *hst3*Δ *hst4*Δ cells, deletion of *DOT1* in a *ctf4*Δ background caused synthetic sensitivity to MMS, whereas *dot1*Δ mutation did not appear to affect the MMS sensitivity of *rtt109*Δ mutants (Figure 6D). These data suggest that lack of H3K79 methylation does not increase cellular resistance to MMS in every mutant of the H3K56Ac pathway.

We verified whether the identified suppressor mutations were able to alleviate the sensitivity of *hst3*Δ *hst4*Δ cells to replicative stress. Epitope tagging of replication enzymes such as Cdc45 causes severe growth defects in *hst3*Δ *hst4*Δ cells, suggesting that these cells are exquisitely sensitive to subtle perturbations of the DNA replication machinery that have essentially no effect on the fitness of WT cells (Celic *et al.* 2008). Remarkably, we found that *sas2*Δ, *dot1*Δ, *H3K79A*, and *H4K16R* mutations partially rescue the slow-growth phenotype of *hst3*Δ *hst4*Δ cells that express Cdc45-HA (Figure 6E). We next sought to assess whether the *H4K16R* or *H3K79R* mutations improved the ability of *hst3*Δ *hst4*Δ mutants to complete DNA replication after transient exposure to MMS (Figure 6F). DNA content analyses by FACS indicated that *hst3*Δ *hst4*Δ *H3K79R* mutant cells replicated a larger fraction of their genome after transient MMS exposure than *hst3*Δ *hst4*Δ cells. The effect of the *H4K16R* mutation was more subtle, although at late time points G_2/M peaks appeared sharper in *hst3*Δ *hst4*Δ *H4K16R* mutants than in *hst3*Δ *hst4*Δ mutants. Taken together, these results indicate that mutations of H4K16 or H3K79 and gene mutations that cripple the acetylation or methylation of these residues all enhance the ability of *hst3*Δ *hst4*Δ cells to survive conditions that induce replicative stress.

We investigated whether reduction of DDR kinase activity would promote completion of DNA replication and survival of *hst3*Δ *hst4*Δ mutants exposed to MMS. *hst3*Δ *hst4*Δ cells were treated with MMS in the presence of caffeine, an inhibitor of the apical DDR kinases Mec1 and Tel1, which are necessary for Rad53 activation (Saiardi *et al.* 2005) . We found that this treatment significantly increased viability compared with the addition of MMS alone (Figure 6G). Moreover, FACS analysis demonstrated that caffeine treatment allowed *hst3*Δ *hst4*Δ cells to complete DNA replication more efficiently in the presence of MMS (Figure 6G). Importantly, the concentration of caffeine used had no effect on the survival of WT cells exposed to MMS (data not shown). These results are consistent with our hypothesis that partial reduction of DDR kinase activity rescues the MMS sensitivity of cells lacking Hst3 and Hst4.

Published reports indicate that mutation of *DOT1* and consequent reduction of DDR kinase activity promote translesion DNA synthesis in response to MMS via molecular mechanisms that remain unclear (Conde *et al.* 2010; Lévesque *et al.* 2010). Interestingly, we found that deletion of *REV3* (encoding the catalytic subunit of DNA polymerase zeta involved in MMS-induced DNA lesion bypass) strongly reduced the suppressive effect of *dot1*Δ, *H4K16R*, and *H3K79R* mutations on the MMS sensitivity of *hst3*Δ *hst4*Δ cells (Figure 6, H and I). This suggests that the aforementioned suppressor mutations may act, at least in part, by promoting DNA damage tolerance via the translesion synthesis pathway in *hst3*Δ *hst4*Δ cells exposed to MMS. However, the *rev3*Δ mutation does not compromise the suppressive effect of *dot1*Δ, *H4K16R*, and *H3K79R* on the Ts- phenotype of *hst3*Δ *hst4*Δ cells (Figure 6, H and I), indicating that this effect is mediated via Rev3-independent pathways.

Links between the temperature and genotoxic agent sensitivity of hst3Δ hst4Δ mutants

The basis of the Ts- phenotype, and its relationship to the genotoxic sensitivity of *hst3*Δ *hst4*Δ mutants are poorly

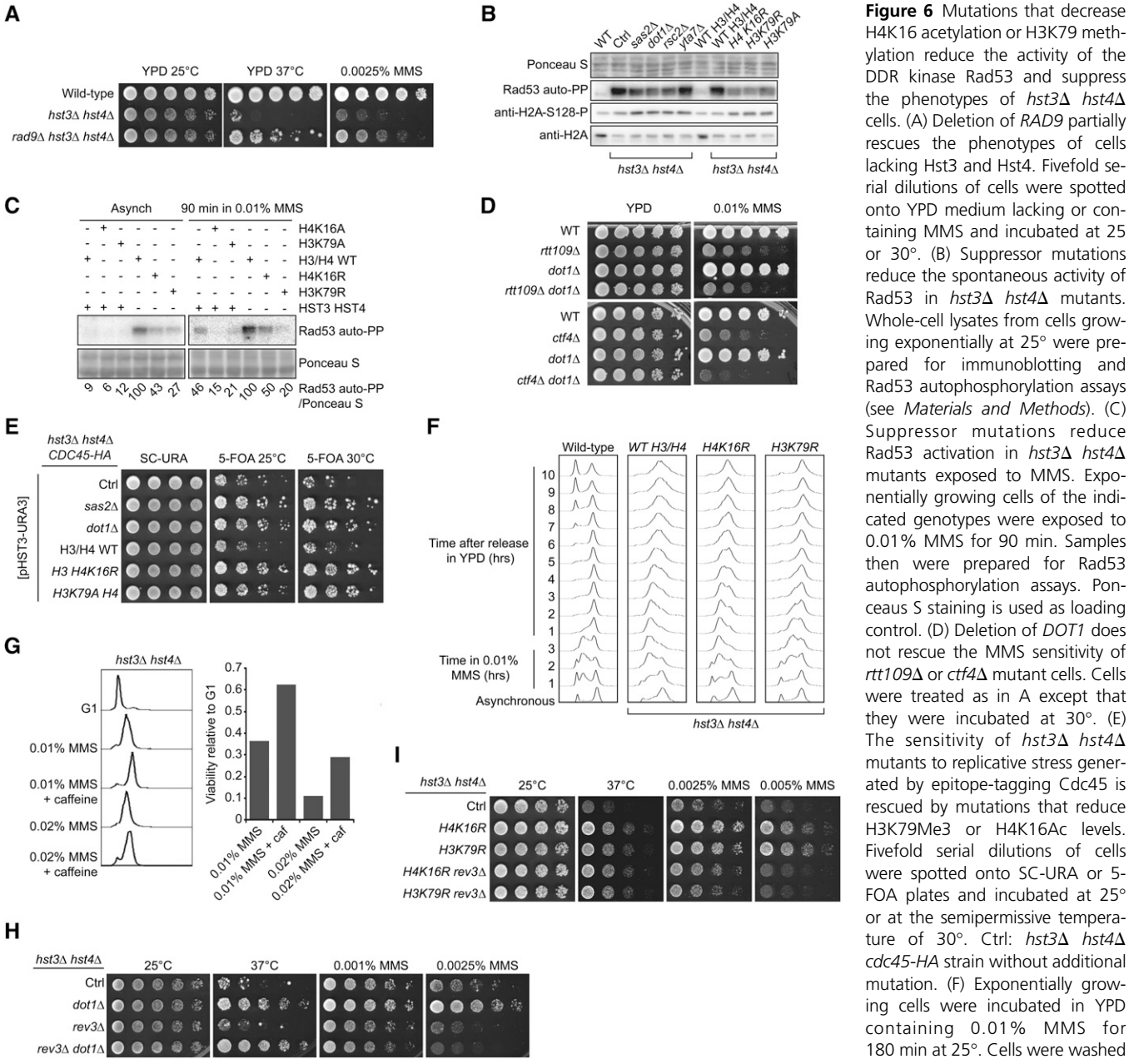

Figure 6 Mutations that decrease H4K16 acetylation or H3K79 methylation reduce the activity of the DDR kinase Rad53 and suppress the phenotypes of *hst3*Δ *hst4*Δ cells. (A) Deletion of *RAD9* partially rescues the phenotypes of cells lacking Hst3 and Hst4. Fivefold serial dilutions of cells were spotted onto YPD medium lacking or containing MMS and incubated at 25 or 30°. (B) Suppressor mutations reduce the spontaneous activity of Rad53 in *hst3*Δ *hst4*Δ mutants. Whole-cell lysates from cells growing exponentially at 25° were prepared for immunoblotting and Rad53 autophosphorylation assays (see *Materials and Methods*). (C) Suppressor mutations reduce Rad53 activation in *hst3*Δ *hst4*Δ mutants exposed to MMS. Exponentially growing cells of the indicated genotypes were exposed to 0.01% MMS for 90 min. Samples then were prepared for Rad53 autophosphorylation assays. Ponceaus S staining is used as loading control. (D) Deletion of *DOT1* does not rescue the MMS sensitivity of *rtt109*Δ or *ctf4*Δ mutant cells. Cells were treated as in A except that they were incubated at 30°. (E) The sensitivity of *hst3*Δ *hst4*Δ mutants to replicative stress generated by epitope-tagging Cdc45 is rescued by mutations that reduce H3K79Me3 or H4K16Ac levels. Fivefold serial dilutions of cells were spotted onto SC-URA or 5-FOA plates and incubated at 25° or at the semipermissive temperature of 30°. Ctrl: *hst3*Δ *hst4*Δ *cdc45-HA* strain without additional mutation. (F) Exponentially growing cells were incubated in YPD containing 0.01% MMS for 180 min at 25°. Cells were washed with YPD containing 2.5% sodium thiosulfate to inactivate MMS and then incubated in YPD. Samples were collected at the indicated times and processed to determine DNA content by FACS. (G) Cells were arrested in G_1 and released into the cell cycle in the presence of the indicated chemicals for 1.5 hr at 25° (right panel). The caffeine concentration was 0.1%. Viability was defined as the ratio of colonies that arose after MMS treatment to colonies formed by G_1 cells that were not exposed to MMS. DNA content was analyzed by FACS for each sample (left panel). (H and I) Deletion of *REV3* compromises the effect of suppressor mutations on the MMS sensitivity of *hst3*Δ *hst4*Δ cells. Fivefold serial dilutions of cells were spotted onto YPD medium lacking or containing MMS and incubated at the indicated temperatures.

understood. We isolated and characterized 12 independent spontaneous suppressors of the Ts- phenotype (see *Materials and Methods*). Aliquots from 12 cultures of *hst3*Δ *hst4*Δ cells carrying a *URA3 CEN* plasmid encoding WT *HST3* were plated on agar medium containing 5-FOA at 37°. This forces surviving cells to lose the plasmid encoding *HST3* and *URA3*, thus selecting for *hst3*Δ *hst4*Δ mutant cells that can form colonies at 37° because they acquire a genetic/epigenetic change that suppresses the Ts- phenotype. We found that only 1 of the 12 thermoresistant (Tr) isolates was as sensitive to chronic MMS exposure as the parental *hst3*Δ *hst4*Δ strain and that two of the Tr isolates were HU sensitive (Figure 7A), demonstrating that the Ts- and genotoxic agent sensitivities of *hst3*Δ *hst4*Δ cells are generally linked.

As mentioned earlier, mutations that prevent H3K56 acetylation partially suppress the phenotypes of *hst3*Δ *hst4*Δ cells

(Celic *et al.* 2006, 2008; Maas *et al.* 2006; Miller *et al.* 2006). Nevertheless, a previous study reported that spontaneous *hst3*Δ *hst4*Δ suppressors rarely manifest reduced H3K56Ac levels (Miller *et al.* 2006). Here we found that H3K56Ac was below detection threshold in only one of the isolated suppressors of the Ts- phenotype (Figure 7B, Tr11). Rtt109 and Asf1 are both required for H3K56 acetylation (Driscoll *et al.* 2007; Han *et al.* 2007b). In order to understand why H3K56Ac was undetectable in this Tr isolate, we epitope-tagged either Rtt109 or Asf1 in this strain. Tr11 showed no decrease in the abundance of Asf1, but the Rtt109-Flag protein was undetectable despite the fact that the *RTT109* gene was appropriately epitope-tagged at its endogenous locus (Figure S3, F and G). Sequencing of the *RTT109* open reading frame in Tr11 revealed a cytosine-to-adenine mutation at position 597 that generates a premature stop codon. We conclude that spontaneous mutation of *RTT109* is a mechanism of phenotypic suppression in *hst3*Δ *hst4*Δ mutants.

The other Tr strains do not generally show strong decreases in H3K56Ac, H4K16 acetylation of H3K79 trimethylation, as assessed by immunoblotting (Figure 7B and Figure S3, A–C). In contrast, most of the Tr isolates that we generated displayed reduction of Rad53 activity and Mec1-mediated histone H2A serine 128 phosphorylation (Figure 7B and Figure S3, D and E). Overall, the data indicate that phenotypic suppression of *hst3*Δ *hst4*Δ is frequently accompanied by a reduction in DDR kinase activity.

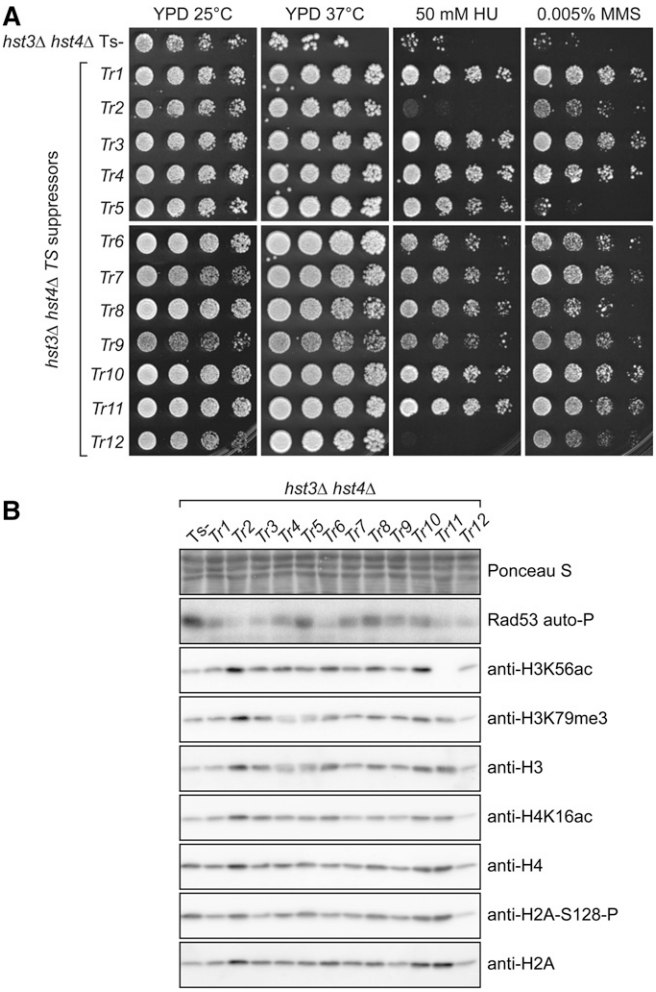

Figure 7 Spontaneous suppressors of *hst3*Δ *hst4*Δ mutant phenotypes exhibit reduced Rad53 activity. (A) Fivefold serial dilutions were spotted on YPD plates containing the indicated concentrations of genotoxic agents and incubated at either 25 or 37°. TS is the starting *hst3*Δ *hst4*Δ mutant strain from which spontaneous thermoresistant (Tr) suppressors were isolated. (B) Immunoblotting was prepared from whole-cell lysates of exponentially growing cells. Ponceau S staining is shown as a loading control.

Discussion

Previous genetic studies established that the temperature and genotoxic drug sensitivity of cells that are incapable of deacetylating H3K56 can be suppressed by secondary mutations (Brachmann *et al.* 1995; Celic *et al.* 2006, 2008) and that interfering with the DNA replication machinery was detrimental to *hst3*Δ *hst4*Δ mutants (Celic *et al.* 2008). Nevertheless, a detailed molecular analysis of the response to replicative stress in *hst3*Δ *hst4*Δ cells was lacking. Here we showed that *hst3*Δ *hst4*Δ cells cannot complete chromosome duplication after transient exposure to MMS or HU during S phase, leading to severe loss of cell viability and formation of persistent Rad52 foci. In general, our results are consistent with studies that reported abnormally high frequencies of spontaneous Rad52 foci in *H3K56R*, *rtt109*Δ, and *hst3*Δ *hst4*Δ mutants (Alvaro *et al.* 2007; Wurtele *et al.* 2012; Muñoz-Galván *et al.* 2013). Recently published data also indicate that replication-associated DNA double-strand breaks (DSBs) require proper levels of H3K56Ac for repair by HR-dependent sister chromatid exchange (SCE) (Muñoz-Galván *et al.* 2013). Based on this, it is possible that persistent Rad52 foci in *hst3*Δ *hst4*Δ mutants transiently exposed to MMS represent abnormal SCE intermediates, which, in turn, could prevent replication restart (Budzowska and Kanaar 2008). Even though our results reveal dysfunctional Rad52 activity in cells lacking Hst3 and Hst4, we previously showed that *hst3*Δ *hst4*Δ *rad52*Δ mutants are not viable (Celic *et al.* 2008). In contrast, the Rad51, Rad54, Rad55, and Rad57 proteins are dispensable for viability of *hst3*Δ *hst4*Δ cells (Celic *et al.* 2008). We speculate that a subset of Rad52-dependent but Rad51-independent HR events may promote survival of *hst3*Δ *hst4*Δ mutants in response to DNA lesions that impede replication and that other Rad52-dependent events (such as SCE) cannot be completed successfully in these mutants (Muñoz-Galván *et al.* 2013). Our observation of anaphase chromatin bridges in a large fraction of *hst3*Δ *hst4*Δ cells containing persistent Rad52 foci (Figure 2B) is consistent with this model. Indeed, such bridges are expected to form in cells that enter anaphase in the presence of incompletely replicated chromosomes and/or unresolved HR structures and have been observed in response to MMS in several replicative stress-sensitive mutants (Germann *et al.* 2014).

Our results clearly show that H3K79 methylation and H4K16 acetylation contribute significantly to the phenotypes

of cells presenting H3K56 hyperacetylation. Interestingly, our immunoblot and mass spectrometry assays indicate that the *H4K16R* mutation reduces global H3K79 trimethylation levels while increasing both mono- and dimethylation at this residue. Potential links between H4K16 acetylation and Dot1-mediated H3K79 methylation have been investigated in previous studies using immunoblotting (Altaf *et al.* 2007; Fingerman *et al.* 2007; Evans *et al.* 2008). Consistent with our mass spectrometry data, Evans *et al.* (2008) found that cells expressing *H4K16R* mutant histones presented elevated levels of mono- and dimethylated H3K79. However, no published study had yet reported decreased global H3K79 trimethylation in *H4K16R* mutants. Dot1-mediated methylation of histone H3 depends on its interaction with a short basic patch of residues in the N-terminal tail of histone H4 (Altaf *et al.* 2007). Current models propose that Dot1 and the Sir3 subunit of the SIR silencing complex compete for binding to this region of H4 and that H4K16 acetylation may promote Dot1-mediated H3K79 methylation by displacing Sir3. Indeed, overexpression of the Sas2 H4K16 acetyltransferase increased the levels of both H4K16Ac and H3K79 trimethylation at subtelomeric regions, suggesting that these two modifications are functionally linked (Altaf *et al.* 2007). Nevertheless, the extent to which reduction in H3K79 trimethylation may contribute to the effect of *H4K16R* mutation on *hst3*Δ *hst4*Δ cells remains unclear. We also recognize that mutations of H3K79 and H4K16 to arginine residues may have consequences that go beyond reduction of their associated histone modifications, although the contribution of modification-independent effects in mediating the phenotypes of *hst3*Δ *hst4*Δ mutants is difficult to assess.

Based on mass spectrometry, it was reported that approximately 85% of H4 molecules are K16 acetylated and 90% of H3 molecules are K79 methylated in asynchronous WT yeast (Smith *et al.* 2002; van Leeuwen *et al.* 2002). Although H4K16Ac and H3K79Me are very abundant in *S. cerevisiae*, they are absent from heterochromatic regions (Kimura *et al.* 2002; Suka *et al.* 2002; van Leeuwen *et al.* 2002; Raisner and Madhani 2008). The boundaries between euchromatin and heterochromatin are characterized by a transition from nucleosomes that contain H4K16Ac/H3K79Me to nucleosomes that lack these modifications. Interestingly, we found that *rsc2*Δ and *yta7*Δ mutations partially suppress the temperature and MMS sensitivity of *hst3*Δ *hst4*Δ cells, albeit to a lesser extent than the *H4K16R* mutation (Figure 5, A–C). Rsc2 and Yta7 have been implicated in preventing heterochromatin spreading, and Yta7 can be detected near chromatin boundaries (Jambunathan *et al.* 2005; Tackett *et al.* 2005; Raisner and Madhani 2008). Although Rsc2 and Yta7 have roles in other processes such as DSB repair (Rsc2) and gene transcription (Yta7) (Kurat *et al.* 2011; Lombardi *et al.* 2011; Chambers *et al.* 2012), it is tempting to speculate that mutations that reduce levels of either H3K79Me and H4K16Ac may suppress the phenotypes of *hst3*Δ *hst4*Δ cells in part by modulating the activity of Rsc2 and Yta7. The precise molecular mechanisms involved are currently unknown. The polypeptide subunits of the Rsc2 complex collectively contain five bromodomains (Yang 2004), which are protein domains involved in binding acetylated lysine residues within specific structural contexts (Filippakopoulos *et al.* 2012), and Yta7 also contains a bromodomain-like domain (Jambunathan *et al.* 2005). It is possible that binding of the RSC complex and/or Yta7 to chromatin containing both H4K16Ac and abnormally elevated stoichiometries of H3K56Ac may interfere with the processing of DNA lesions that impede replication (*e.g.*, MMS-induced 3-methyladenine). Alternatively, abnormal expression of specific genes as a result of crippled chromatin boundaries may partly account for the effect of *RSC2* or *YTA7* deletion on the phenotypes of *hst3*Δ *hst4*Δ cells. Further studies will be required to investigate the validity of these models.

Our data provide compelling evidence in support of a role for H4K16Ac and H3K79Me in promoting persistent activation of DDR signaling in *hst3*Δ *hst4*Δ cells (Figure 6). H3K79 methylation is critical for chromatin binding and optimal activation of the Rad9 adaptor protein, which, in turn, permits full activation of the kinase Rad53 in response to DNA damage (Wysocki *et al.* 2005; Javaheri *et al.* 2006; Toh *et al.* 2006; Grenon *et al.* 2007). Based on four main lines of evidence, we propose that this function of H3K79 methylation is deleterious to *hst3*Δ *hst4*Δ mutants. In *hst3*Δ *hst4*Δ cells, (1) reduction of H3K79Me, via mutations of the Dot1 methyltransferase or H3K79R, decreases spontaneous and MMS-induced Rad53 activation (Figure 6, B and C), (2) deletion of *RAD9* itself partially suppresses the temperature and genotoxic drug sensitivity (Figure 6A), (3) caffeine treatment markedly alleviates the lethality induced by MMS (Figure 6G), and (4) several spontaneous suppressors of the Ts- phenotype display reduced activation of the kinase Rad53 (Figure 7B). This interpretation is also consistent with our previously published observations indicating that a null mutation of *RAD24*, encoding the large subunits of a replication factor C-related complex responsible for loading the PCNA-like 9-1-1 complex, suppresses the Ts- phenotype of *hst3*Δ *hst4*Δ mutants (Celic *et al.* 2008). Similarly, mutation of the genes encoding the three 9-1-1 subunits (*MEC3*, *DDC1*, and *RAD17*) also suppress the Ts- phenotype of *hst3*Δ *hst4*Δ mutants without decreasing H3K56Ac (Celic *et al.* 2008). Since loading of 9-1-1 clamps at sites of DNA damage promotes DNA damage checkpoint activation (Parrilla-Castellar *et al.* 2004), these genetic data are consistent with the notion that persistent activation of DDR kinases is detrimental to the survival *of hst3*Δ *hst4*Δ mutants.

It seems plausible that persistent activation of DDR kinases may contribute to the phenotypes of *hst3*Δ *hst4*Δ mutants through various mechanisms that are not mutually exclusive. For example, a well-known function of Rad53 is to inhibit the firing of late DNA replication origins (Santocanale and Diffley 1998; Zegerman and Diffley 2007). Persistent activity of DDR kinases in *hst3*Δ *hst4*Δ cells transiently exposed to MMS could inhibit the firing of at least a subset of late DNA

replication origins, thus preventing cells from completing replication where forks are permanently blocked by MMS lesions. Our results also argue that Rad53-mediated inhibition of translesion DNA synthesis (TLS) contributes to the MMS sensitivity of *hst3*Δ *hst4*Δ mutants (Figure 6, H and I). These data are in line with published results showing that reduction of DDR kinase activity and concomitant increase in TLS partially suppress the MMS sensitivity caused by deletion of genes such as *RAD52* or *RTT107*(Conde and San-Segundo 2008; Conde *et al.* 2010; Lévesque *et al.* 2010). Interestingly, deletion of the *REV3* gene encoding the catalytic subunit of translesion DNA polymerase zeta does not influence suppression of the Ts- phenotype of *hst3*Δ *hst4*Δ cells by *dot1*Δ, *H3K79R*, or *H4K16R* (Figure 6, H and I). Further studies will be required to identify the mechanisms through which these mutations suppress the Ts- phenotype of *hst3*Δ *hst4*Δ mutants because its molecular basis remains poorly understood.

In fission yeast and human cells, the vast majority of histone H4 molecules are methylated at lysine 20 (H4K20Me) (Drogaris *et al.* 2012; A. Verreault, unpublished results), a modification whose role in the DDR is functionally related to that of *S. cerevisiae* H3K79Me. Indeed, orthologs of Rad9 in fission yeast (Crb2) and humans (53BP1) have been reported to interact with H4K20Me, which demonstrates an evolutionarily conserved link between histone methylation and DNA damage–induced signaling (Botuyan *et al.* 2006; Du *et al.* 2006; Xie *et al.* 2007). Taken together, our results suggest that in addition to abundant modifications such as H4K20Me in *S. pombe* and human cells or H3K79Me in *S. cerevisiae*, genome-wide deacetylation of newly synthesized histones (H3K56Ac in *S. cerevisiae* and *S. pombe* and, possibly, N-terminal acetylation sites of H3 and H4 in human cells) may be critical for appropriate regulation of DDR kinases and cell survival in response to DNA damage.

Acknowledgments

We thank Francis Fabre (Centre National de la Recherche Scientifique, France) for *MAT***a** and *MATα* expression plasmids and Stephen Bell (MIT, USA) for the *CDC45-HA3* integration vector. We also thank Edlie St-Hilaire for her excellent technical support and Jean-Claude Labbé and Elliot Drobetsky for critical reading of our manuscript. This work was supported by grants from the Canadian Institutes for Health Research to H.W. (MOP 123438) and A.V. (MOP 89928 and IC1-123780), a Natural Sciences and Engineering Research Council grant to P.T. (NSERC 311598), a Natural Sciences and Engineering Research Council of Canada (NSERC) grant to S.C. and an NIH grant to J.D.B (U54 GM-103520). H.W. is the recipient of a Fonds de la recherche du Québec-Santé Junior 1 scholarship and is supported by the Maisonneuve-Rosemont Hospital Foundation. S.C. is the recipient of a Fonds de la Recherche du Québec-Santé Junior 2 scholarship. A.S. is the recipient of a PhD scholarship from the Fonds de la recherche du Québec-Santé. N.D. was the recipient of a Ph.D. award from the Cole Foundation. IRIC receives infrastructure support from IRICoR, the Canadian Foundation for Innovation and the Fonds de Recherche du Québéc–Santé (FRQS).

Literature Cited

Alabert, C., J. N. Bianco, and P. Pasero, 2009 Differential regulation of homologous recombination at DNA breaks and replication forks by the Mrc1 branch of the S-phase checkpoint. EMBO J. 28: 1131–1141.

Alcasabas, A. A., A. J. Osborn, J. Bachant, F. Hu, P. J. Werler *et al.*, 2001 Mrc1 transduces signals of DNA replication stress to activate Rad53. Nat. Cell Biol. 3: 958–965.

Altaf, M., R. T. Utley, N. Lacoste, S. Tan, S. D. Briggs *et al.*, 2007 Interplay of chromatin modifiers on a short basic patch of histone H4 tail defines the boundary of telomeric heterochromatin. Mol. Cell 28: 1002–1014.

Alvaro, D., M. Lisby, and R. Rothstein, 2007 Genome-wide analysis of Rad52 foci reveals diverse mechanisms impacting recombination. PLoS Genet. 3: e228.

Aparicio, O. M., D. M. Weinstein, and S. P. Bell, 1997 Components and dynamics of DNA replication complexes in S. cerevisiae: redistribution of MCM proteins and Cdc45p during S phase. Cell 91: 59–69.

Barbour, L., and W. Xiao, 2006 Mating type regulation of cellular tolerance to DNA damage is specific to the DNA post-replication repair and mutagenesis pathway. Mol. Microbiol. 59: 637–650.

Benson, L. J., Y. Gu, T. Yakovleva, K. Tong, C. Barrows *et al.*, 2006 Modifications of H3 and H4 during chromatin replication, nucleosome assembly, and histone exchange. J. Biol. Chem. 281: 9287–9296.

Beranek, D. T., R. H. Heflich, R. L. Kodell, S. M. Morris, and D. A. Casciano, 1983 Correlation between specific DNA-methylation products and mutation induction at the HGPRT locus in Chinese hamster ovary cells. Mutat. Res. 110: 171–180.

Botuyan, M. V., J. Lee, I. M. Ward, J.-E. Kim, J. R. Thompson *et al.*, 2006 Structural basis for the methylation state-specific recognition of histone H4–K20 by 53BP1 and Crb2 in DNA repair. Cell 127: 1361–1373.

Brachmann, C. B., J. M. Sherman, S. E. Devine, E. E. Cameron, L. Pillus *et al.*, 1995 The SIR2 gene family, conserved from bacteria to humans, functions in silencing, cell cycle progression, and chromosome stability. Genes Dev. 9: 2888–2902.

Branzei, D., and M. Foiani, 2009 The checkpoint response to replication stress. DNA Repair 8: 1038–1046.

Brill, S. J., and B. Stillman, 1991 Replication factor-A from Saccharomyces cerevisiae is encoded by three essential genes coordinately expressed at S phase. Genes Dev. 5: 1589–1600.

Budzowska, M., and R. Kanaar, 2008 Mechanisms of dealing with DNA damage-induced replication problems. Cell Biochem. Biophys. 53: 17–31.

Burgess, R. J., H. Zhou, J. Han, and Z. Zhang, 2010 A role for Gcn5 in replication-coupled nucleosome assembly. Mol. Cell 37: 469–480.

Cairns, B. R., A. Schlichter, H. Erdjument-Bromage, P. Tempst, R. D. Kornberg *et al.*, 1999 Two functionally distinct forms of the RSC nucleosome-remodeling complex, containing essential AT hook, BAH, and bromodomains. Mol. Cell 4: 715–723.

Campos, E. I., and D. Reinberg, 2009 Histones: annotating chromatin. Annu. Rev. Genet. 43: 559–599.

Celic, I., H. Masumoto, W. P. Griffith, P. Meluh, R. J. Cotter *et al.*, 2006 The sirtuins hst3 and Hst4p preserve genome integrity by controlling histone h3 lysine 56 deacetylation. Curr. Biol. 16: 1280–1289.

Celic, I., A. Verreault, and J. D. Boeke, 2008 Histone H3 K56 hyperacetylation perturbs replisomes and causes DNA damage. Genetics 179: 1769–1784.
Chambers, A. L., P. M. Brownlee, S. C. Durley, T. Beacham, N. A. Kent *et al.*, 2012 The two different isoforms of the RSC chromatin remodeling complex play distinct roles in DNA damage responses. PLoS ONE 7: e32016.
Clapier, C. R., and B. R. Cairns, 2009 The biology of chromatin remodeling complexes. Annu. Rev. Biochem. 78: 273–304.
Collins, S. R., K. M. Miller, N. L. Maas, A. Roguev, J. Fillingham *et al.*, 2007 Functional dissection of protein complexes involved in yeast chromosome biology using a genetic interaction map. Nature 446: 806–810.
Conde, F., D. Ontoso, I. Acosta, A. Gallego-Sánchez, A. Bueno *et al.*, 2010 Regulation of tolerance to DNA alkylating damage by Dot1 and Rad53 in Saccharomyces cerevisiae. DNA Repair 9: 1038–1049.
Conde, F., and P. A. San-Segundo, 2008 Role of Dot1 in the response to alkylating DNA damage in *Saccharomyces cerevisiae*: regulation of DNA damage tolerance by the error-prone polymerases Polζ/Rev1. Genetics 179: 1197–1210.
Dang, W., K. K. Steffen, R. Perry, J. A. Dorsey, F. B. Johnson *et al.*, 2009 Histone H4 lysine 16 acetylation regulates cellular lifespan. Nature 459: 802–807.
Downs, J. A., N. F. Lowndes, and S. P. Jackson, 2000 A role for *Saccharomyces cerevisiae* histone H2A in DNA repair. Nature 408: 1001–1004.
Driscoll, R., A. Hudson, and S. P. Jackson, 2007 Yeast Rtt109 promotes genome stability by acetylating histone H3 on lysine 56. Science 315: 649–652.
Drogaris, P., V. Villeneuve, C. Pomiès, E.-H. Lee, V. Bourdeau *et al.*, 2012 Histone deacetylase inhibitors globally enhance h3/h4 tail acetylation without affecting h3 lysine 56 acetylation. Sci. Rep. 2: 220.
Drogaris, P., H. Wurtele, H. Masumoto, A. Verreault, and P. Thibault, 2008 Comprehensive profiling of histone modifications using a label-free approach and its applications in determining structure-function relationships. Anal. Chem. 80: 6698–6707.
Du, L.-L., T. M. Nakamura, and P. Russell, 2006 Histone modification-dependent and -independent pathways for recruitment of checkpoint protein Crb2 to double-strand breaks. Genes Dev. 20: 1583–1596.
Evans, M. L., L. J. Bostelman, A. M. Albrecht, A. M. Keller, N. T. Strande *et al.*, 2008 UV sensitive mutations in histone H3 in *Saccharomyces cerevisiae* that alter specific K79 methylation states genetically act through distinct DNA repair pathways. Curr. Genet. 53: 259–274.
Filippakopoulos, P., S. Picaud, M. Mangos, T. Keates, J.-P. Lambert *et al.*, 2012 Histone recognition and large-scale structural analysis of the human bromodomain family. Cell 149: 214–231.
Fingerman, I. M., H.-C. Li, and S. D. Briggs, 2007 A charge-based interaction between histone H4 and Dot1 is required for H3K79 methylation and telomere silencing: identification of a new trans-histone pathway. Genes Dev. 21: 2018–2029.
Floer, M., X. Wang, V. Prabhu, G. Berrozpe, S. Narayan *et al.*, 2010 A RSC/nucleosome complex determines chromatin architecture and facilitates activator binding. Cell 141: 407–418.
Germann, S. M., V. Schramke, R. T. Pedersen, I. Gallina, N. Eckert-Boulet *et al.*, 2014 TopBP1/Dpb11 binds DNA anaphase bridges to prevent genome instability. J. Cell Biol. 204: 45–59.
Grenon, M., T. Costelloe, S. Jimeno, A. O'Shaughnessy, J. Fitzgerald *et al.*, 2007 Docking onto chromatin via the *Saccharomyces cerevisiae* Rad9 Tudor domain. Yeast 24: 105–119.
Guillemette, B., P. Drogaris, H.-H. S. Lin, H. Armstrong, K. Hiragami-Hamada *et al.*, 2011 H3 lysine 4 is acetylated at active gene promoters and is regulated by H3 lysine 4 methylation. PLoS Genet. 7: e1001354.
Gunjan, A., and A. Verreault, 2003 A Rad53 kinase-dependent surveillance mechanism that regulates histone protein levels in S. cerevisiae. Cell 115: 537–549.
Haase, S. B., and S. I. Reed, 2002 Improved flow cytometric analysis of the budding yeast cell cycle. Cell Cycle 1: 132–136.
Hachinohe, M., F. Hanaoka, and H. Masumoto, 2011 Hst3 and Hst4 histone deacetylases regulate replicative lifespan by preventing genome instability in *Saccharomyces cerevisiae*. Genes Cells Devoted Mol. Cell. Mech. 16: 467–477.
Haldar, D., and R. T. Kamakaka, 2008 *Schizosaccharomyces pombe* Hst4 functions in DNA damage response by regulating histone H3 K56 acetylation. Eukaryot. Cell 7: 800–813.
Han, J., H. Zhou, B. Horazdovsky, K. Zhang, R.-M. Xu *et al.*, 2007a Rtt109 acetylates histone H3 lysine 56 and functions in DNA replication. Science 315: 653–655.
Han, J., H. Zhou, Z. Li, R.-M. Xu, and Z. Zhang, 2007b Acetylation of lysine 56 of histone H3 catalyzed by RTT109 and regulated by ASF1 is required for replisome integrity. J. Biol. Chem. 282: 28587–28596.
Han, J., H. Zhang, H. Zhang, Z. Wang, H. Zhou *et al.*, 2013 A Cul4 E3 ubiquitin ligase regulates histone hand-off during nucleosome assembly. Cell 155: 817–829.
Hoppe, G. J., J. C. Tanny, A. D. Rudner, S. A. Gerber, S. Danaie *et al.*, 2002 Steps in assembly of silent chromatin in yeast: Sir3-independent binding of a Sir2/Sir4 complex to silencers and role for Sir2-dependent deacetylation. Mol. Cell. Biol. 22: 4167–4180.
Hyland, E. M., M. S. Cosgrove, H. Molina, D. Wang, A. Pandey *et al.*, 2005 Insights into the role of histone H3 and histone H4 core modifiable residues in *Saccharomyces cerevisiae*. Mol. Cell. Biol. 25: 10060–10070.
Imai, S., C. M. Armstrong, M. Kaeberlein, and L. Guarente, 2000 Transcriptional silencing and longevity protein Sir2 is an NAD-dependent histone deacetylase. Nature 403: 795–800.
Ito-Harashima, S., and J. H. McCusker, 2004 Positive and negative selection LYS5MX gene replacement cassettes for use in *Saccharomyces cerevisiae*. Yeast 21: 53–61.
Jackson, V., A. Shires, N. Tanphaichitr, and R. Chalkley, 1976 Modifications to histones immediately after synthesis. J. Mol. Biol. 104: 471–483.
Jambunathan, N., A. W. Martinez, E. C. Robert, N. B. Agochukwu, M. E. Ibos *et al.*, 2005 Multiple bromodomain genes are involved in restricting the spread of heterochromatic silencing at the *Saccharomyces cerevisiae* HMR-tRNA boundary. Genetics 171: 913–922.
Jasencakova, Z., A. N. D. Scharf, K. Ask, A. Corpet, A. Imhof *et al.*, 2010 Replication stress interferes with histone recycling and predeposition marking of new histones. Mol. Cell 37: 736–743.
Javaheri, A., R. Wysocki, O. Jobin-Robitaille, M. Altaf, J. Côté *et al.*, 2006 Yeast G_1 DNA damage checkpoint regulation by H2A phosphorylation is independent of chromatin remodeling. Proc. Natl. Acad. Sci. USA 103: 13771–13776.
Kaplan, T., C. L. Liu, J. A. Erkmann, J. Holik, M. Grunstein *et al.*, 2008 Cell cycle- and chaperone-mediated regulation of H3K56ac incorporation in yeast. PLoS Genet. 4: e1000270.
Kimura, A., T. Umehara, and M. Horikoshi, 2002 Chromosomal gradient of histone acetylation established by Sas2p and Sir2p functions as a shield against gene silencing. Nat. Genet. 32: 370–377.
Kouprina, N., E. Kroll, V. Bannikov, V. Bliskovsky, R. Gizatullin *et al.*, 1992 CTF4 (CHL15) mutants exhibit defective DNA metabolism in the yeast *Saccharomyces cerevisiae*. Mol. Cell. Biol. 12: 5736–5747.
Krogh, B. O., and L. S. Symington, 2004 Recombination Proteins in Yeast. Annu. Rev. Genet. 38: 233–271.
Kurat, C. F., J.-P. Lambert, D. van Dyk, K. Tsui, H. van Bakel *et al.*, 2011 Restriction of histone gene transcription to S phase by

phosphorylation of a chromatin boundary protein. Genes Dev. 25: 2489–2501.
Kushnirov, V. V., 2000 Rapid and reliable protein extraction from yeast. Yeast 16: 857–860.
Landry, J., A. Sutton, S. T. Tafrov, R. C. Heller, J. Stebbins *et al.*, 2000 The silencing protein SIR2 and its homologs are NAD-dependent protein deacetylases. Proc. Natl. Acad. Sci. USA 97: 5807–5811.
van Leeuwen, F., P. R. Gafken, and D. E. Gottschling, 2002 Dot1p modulates silencing in yeast by methylation of the nucleosome core. Cell 109: 745–756.
Lévesque, N., G. P. Leung, A. K. Fok, T. I. Schmidt, and M. S. Kobor, 2010 Loss of H3 K79 trimethylation leads to suppression of Rtt107-dependent DNA damage sensitivity through the translesion synthesis pathway. J. Biol. Chem. 285: 35113–35122.
Li, Q., and Z. Zhang, 2012 Linking DNA replication to heterochromatin silencing and epigenetic inheritance. Acta Biochim. Biophys. Sin. 44: 3–13.
Li, Q., H. Zhou, H. Wurtele, B. Davies, B. Horazdovsky *et al.*, 2008 Acetylation of histone H3 lysine 56 regulates replication-coupled nucleosome assembly. Cell 134: 244–255.
Lisby, M., J. H. Barlow, R. C. Burgess, and R. Rothstein, 2004 Choreography of the DNA damage response: spatiotemporal relationships among checkpoint and repair proteins. Cell 118: 699–713.
Livi, G. P., and V. L. Mackay, 1980 Mating-type regulation of methyl methanesulfonate sensitivity in *Saccharomyces cerevisiae*. Genetics 95: 259–271.
Lombardi, L. M., A. Ellahi, and J. Rine, 2011 Direct regulation of nucleosome density by the conserved AAA-ATPase Yta7. Proc. Natl. Acad. Sci. USA 108: E1302–E1311.
Maas, N. L., K. M. Miller, L. G. DeFazio, and D. P. Toczyski, 2006 Cell cycle and checkpoint regulation of histone H3 K56 acetylation by Hst3 and Hst4. Mol. Cell 23: 109–119.
Maringele, L., and D. Lydall, 2006 Pulsed-field gel electrophoresis of budding yeast chromosomes. Methods Mol. Biol. 313: 65–73.
Masai, H., S. Matsumoto, Z. You, N. Yoshizawa-Sugata, and M. Oda, 2010 Eukaryotic chromosome DNA replication: where, when, and how? Annu. Rev. Biochem. 79: 89–130.
Masumoto, H., D. Hawke, R. Kobayashi, and A. Verreault, 2005 A role for cell-cycle-regulated histone H3 lysine 56 acetylation in the DNA damage response. Nature 436: 294–298.
Miller, K. M., N. L. Maas, and D. P. Toczyski, 2006 Taking it off: regulation of H3 K56 acetylation by Hst3 and Hst4. Cell Cycle 5: 2561–2565.
Muñoz-Galván, S., S. Jimeno, R. Rothstein, and A. Aguilera, 2013 Histone H3K56 acetylation, Rad52, and non-DNA repair factors control double-strand break repair choice with the sister chromatid. PLoS Genet. 9: e1003237.
Nakanishi, S., B. W. Sanderson, K. M. Delventhal, W. D. Bradford, K. Staehling-Hampton *et al.*, 2008 A comprehensive library of histone mutants identifies nucleosomal residues required for H3K4 methylation. Nat. Struct. Mol. Biol. 15: 881–888.
Nguyen, A. T., and Y. Zhang, 2011 The diverse functions of Dot1 and H3K79 methylation. Genes Dev. 25: 1345–1358.
Osborn, A. J., and S. J. Elledge, 2003 Mrc1 is a replication fork component whose phosphorylation in response to DNA replication stress activates Rad53. Genes Dev. 17: 1755–1767.
Ozdemir, A., S. Spicuglia, E. Lasonder, M. Vermeulen, C. Campsteijn *et al.*, 2005 Characterization of lysine 56 of histone H3 as an acetylation site in Saccharomyces cerevisiae. J. Biol. Chem. 280: 25949–25952.
Park, J.-H., M. S. Cosgrove, E. Youngman, C. Wolberger, and J. D. Boeke, 2002 A core nucleosome surface crucial for transcriptional silencing. Nat. Genet. 32: 273–279.
Parrilla-Castellar, E. R., S. J. H. Arlander, and L. Karnitz, 2004 Dial 9-1-1 for DNA damage: the Rad9-Hus1-Rad1 (9-1-1) clamp complex. DNA Repair 3: 1009–1014.
Parthun, M. R., J. Widom, and D. E. Gottschling, 1996 The major cytoplasmic histone acetyltransferase in yeast: links to chromatin replication and histone metabolism. Cell 87: 85–94.
Pellicioli, A., and M. Foiani, 2005 Signal transduction: how Rad53 kinase is activated. Curr. Biol. 15: R769–R771.
Pellicioli, A., C. Lucca, G. Liberi, F. Marini, M. Lopes *et al.*, 1999 Activation of Rad53 kinase in response to DNA damage and its effect in modulating phosphorylation of the lagging strand DNA polymerase. EMBO J. 18: 6561–6572.
Raisner, R. M., and H. D. Madhani, 2008 Genomewide screen for negative regulators of sirtuin activity in *Saccharomyces cerevisiae* reveals 40 loci and links to metabolism. Genetics 179: 1933–1944.
Ransom, M., B. K. Dennehey, and J. K. Tyler, 2010 Chaperoning histones during DNA replication and repair. Cell 140: 183–195.
Recht, J., T. Tsubota, J. C. Tanny, R. L. Diaz, J. M. Berger *et al.*, 2006 Histone chaperone Asf1 is required for histone H3 lysine 56 acetylation, a modification associated with S phase in mitosis and meiosis. Proc. Natl. Acad. Sci. USA 103: 6988–6993.
Reid, R. J. D., S. González-Barrera, I. Sunjevaric, D. Alvaro, S. Ciccone *et al.*, 2011 Selective ploidy ablation, a high-throughput plasmid transfer protocol, identifies new genes affecting topoisomerase I-induced DNA damage. Genome Res. 21: 477–486.
Ruiz-Carrillo, A., L. J. Wangh, and V. G. Allfrey, 1975 Processing of newly synthesized histone molecules. Science 190: 117–128.
Saiardi, A., A. C. Resnick, A. M. Snowman, B. Wendland, and S. H. Snyder, 2005 Inositol pyrophosphates regulate cell death and telomere length through phosphoinositide 3-kinase-related protein kinases. Proc. Natl. Acad. Sci. USA 102: 1911–1914.
Santocanale, C., and J. F. Diffley, 1998 A Mec1- and Rad53-dependent checkpoint controls late-firing origins of DNA replication. Nature 395: 615–618.
Schneider, J., P. Bajwa, F. C. Johnson, S. R. Bhaumik, and A. Shilatifard, 2006 Rtt109 is required for proper H3K56 acetylation: a chromatin mark associated with the elongating RNA polymerase II. J. Biol. Chem. 281: 37270–37274.
Smith, J. S., C. B. Brachmann, I. Celic, M. A. Kenna, S. Muhammad *et al.*, 2000 A phylogenetically conserved NAD^+-dependent protein deacetylase activity in the Sir2 protein family. Proc. Natl. Acad. Sci. USA 97: 6658–6663.
Smith, J. S., C. B. Brachmann, L. Pillus, and J. D. Boeke, 1998 Distribution of a limited Sir2 protein pool regulates the strength of yeast rDNA silencing and is modulated by Sir4p. Genetics 149: 1205–1219.
Smith, C. M., Z. W. Haimberger, C. O. Johnson, A. J. Wolf, P. R. Gafken *et al.*, 2002 Heritable chromatin structure: mapping "memory" in histones H3 and H4. Proc. Natl. Acad. Sci. USA 99(Suppl. 4): 16454–16461.
Su, D., Q. Hu, Q. Li, J. R. Thompson, G. Cui, A. Fazly, B. A. Davies, M. V. Botuyan, Z. Zhang, and G. Mer, 2012 Structural basis for recognition of H3K56-acetylated histone H3–H4 by the chaperone Rtt106. Nature 483: 104–107.
Suka, N., K. Luo, and M. Grunstein, 2002 Sir2p and Sas2p oppositely regulate acetylation of yeast histone H4 lysine16 and spreading of heterochromatin. Nat. Genet. 32: 378–383.
Sutton, A., W.-J. Shia, D. Band, P. D. Kaufman, S. Osada *et al.*, 2003 Sas4 and Sas5 are required for the histone acetyltransferase activity of Sas2 in the SAS complex. J. Biol. Chem. 278: 16887–16892.
Sweeney, F. D., F. Yang, A. Chi, J. Shabanowitz, D. F. Hunt *et al.*, 2005 Saccharomyces cerevisiae Rad9 acts as a Mec1 adaptor to allow Rad53 activation. Curr. Biol. 15: 1364–1375.

Tackett, A. J., D. J. Dilworth, M. J. Davey, M. O'Donnell, J. D. Aitchison *et al.*, 2005 Proteomic and genomic characterization of chromatin complexes at a boundary. J. Cell Biol. 169: 35–47.

Taddei, A., D. Roche, J. B. Sibarita, B. M. Turner, and G. Almouzni, 1999 Duplication and maintenance of heterochromatin domains. J. Cell Biol. 147: 1153–1166.

Tang, Y., M. A. Holbert, H. Wurtele, K. Meeth, W. Rocha *et al.*, 2008 Fungal Rtt109 histone acetyltransferase is an unexpected structural homolog of metazoan p300/CBP. Nat. Struct. Mol. Biol. 15: 738–745.

Tanny, J. C., and D. Moazed, 2001 Coupling of histone deacetylation to NAD breakdown by the yeast silencing protein Sir2: evidence for acetyl transfer from substrate to an NAD breakdown product. Proc. Natl. Acad. Sci. USA 98: 415–420.

Thaminy, S., B. Newcomb, J. Kim, T. Gatbonton, E. Foss *et al.*, 2007 Hst3 is regulated by Mec1-dependent proteolysis and controls the S phase checkpoint and sister chromatid cohesion by deacetylating histone H3 at lysine 56. J. Biol. Chem. 282: 37805–37814.

Thorpe, P. H., D. Alvaro, M. Lisby, and R. Rothstein, 2011 Bringing Rad52 foci into focus. J. Cell Biol. 194: 665–667.

Toh, G. W.-L., A. M. O'Shaughnessy, S. Jimeno, I. M. Dobbie, M. Grenon *et al.*, 2006 Histone H2A phosphorylation and H3 methylation are required for a novel Rad9 DSB repair function following checkpoint activation. DNA Repair 5: 693–703.

Tsubota, T., C. E. Berndsen, J. A. Erkmann, C. L. Smith, L. Yang *et al.*, 2007 Histone H3–K56 acetylation is catalyzed by histone chaperone-dependent complexes. Mol. Cell 25: 703–712.

Winston, F., C. Dollard, and S. L. Ricupero-Hovasse, 1995 Construction of a set of convenient *Saccharomyces cerevisiae* strains that are isogenic to S288C. Yeast 11: 53–55.

Wurtele, H., G. S. Kaiser, J. Bacal, E. St-Hilaire, E.-H. Lee *et al.*, 2012 Histone H3 lysine 56 acetylation and the response to DNA replication fork damage. Mol. Cell. Biol. 32: 154–172.

Wurtele, H., S. Tsao, G. Lepine, A. Mullick, J. Tremblay *et al.*, 2010 Modulation of histone H3 lysine 56 acetylation as an antifungal therapeutic strategy. Nat. Med. 16: 774–780.

Wurtele, H., and A. Verreault, 2006 Histone post-translational modifications and the response to DNA double-strand breaks. Curr. Opin. Cell Biol. 18: 137–144.

Wysocki, R., A. Javaheri, S. Allard, F. Sha, J. Côté *et al.*, 2005 Role of Dot1-dependent histone H3 methylation in G1 and S phase DNA damage checkpoint functions of Rad9. Mol. Cell. Biol. 25: 8430–8443.

Xie, A., A. Hartlerode, M. Stucki, S. Odate, N. Puget *et al.*, 2007 Distinct roles of chromatin-associated proteins MDC1 and 53BP1 in mammalian double-strand break repair. Mol. Cell 28: 1045–1057.

Xu, F., K. Zhang, and M. Grunstein, 2005 Acetylation in histone H3 globular domain regulates gene expression in yeast. Cell 121: 375–385.

Xu, F., Q. Zhang, K. Zhang, W. Xie, and M. Grunstein, 2007 Sir2 deacetylates histone H3 lysine 56 to regulate telomeric heterochromatin structure in yeast. Mol. Cell 27: 890–900.

Yang, X.-J., 2004 Lysine acetylation and the bromodomain: a new partnership for signaling. Bioessays 26: 1076–1087.

Yang, B., A. Miller, and A. L. Kirchmaier, 2008 HST3/HST4-dependent deacetylation of lysine 56 of histone H3 in silent chromatin. Mol. Biol. Cell 19: 4993–5005.

Yarbro, J. W., 1992 Mechanism of action of hydroxyurea. Semin. Oncol. 19: 1–10.

Ye, J., X. Ai, E. E. Eugeni, L. Zhang, L. R. Carpenter *et al.*, 2005 Histone H4 lysine 91 acetylation a core domain modification associated with chromatin assembly. Mol. Cell 18: 123–130.

Zegerman, P., and J. F. X. Diffley, 2007 Phosphorylation of Sld2 and Sld3 by cyclin-dependent kinases promotes DNA replication in budding yeast. Nature 445: 281–285.

Zou, L., and S. J. Elledge, 2003 Sensing DNA damage through ATRIP recognition of RPA-ssDNA complexes. Science 300: 1542–1548.

Communicating editor: J. A. Nickoloff

GENETICS

Supporting Information
http://www.genetics.org/lookup/suppl/doi:10.1534/genetics.115.175919/-/DC1

Interplay Between Histone H3 Lysine 56 Deacetylation and Chromatin Modifiers in Response to DNA Damage

Antoine Simoneau, Neda Delgoshaie, Ivana Celic, Junbiao Dai, Nebiyu Abshiru, Santiago Costantino, Pierre Thibault, Jef D. Boeke, Alain Verreault, and Hugo Wurtele

DOI: 10.1534/genetics.115.175919

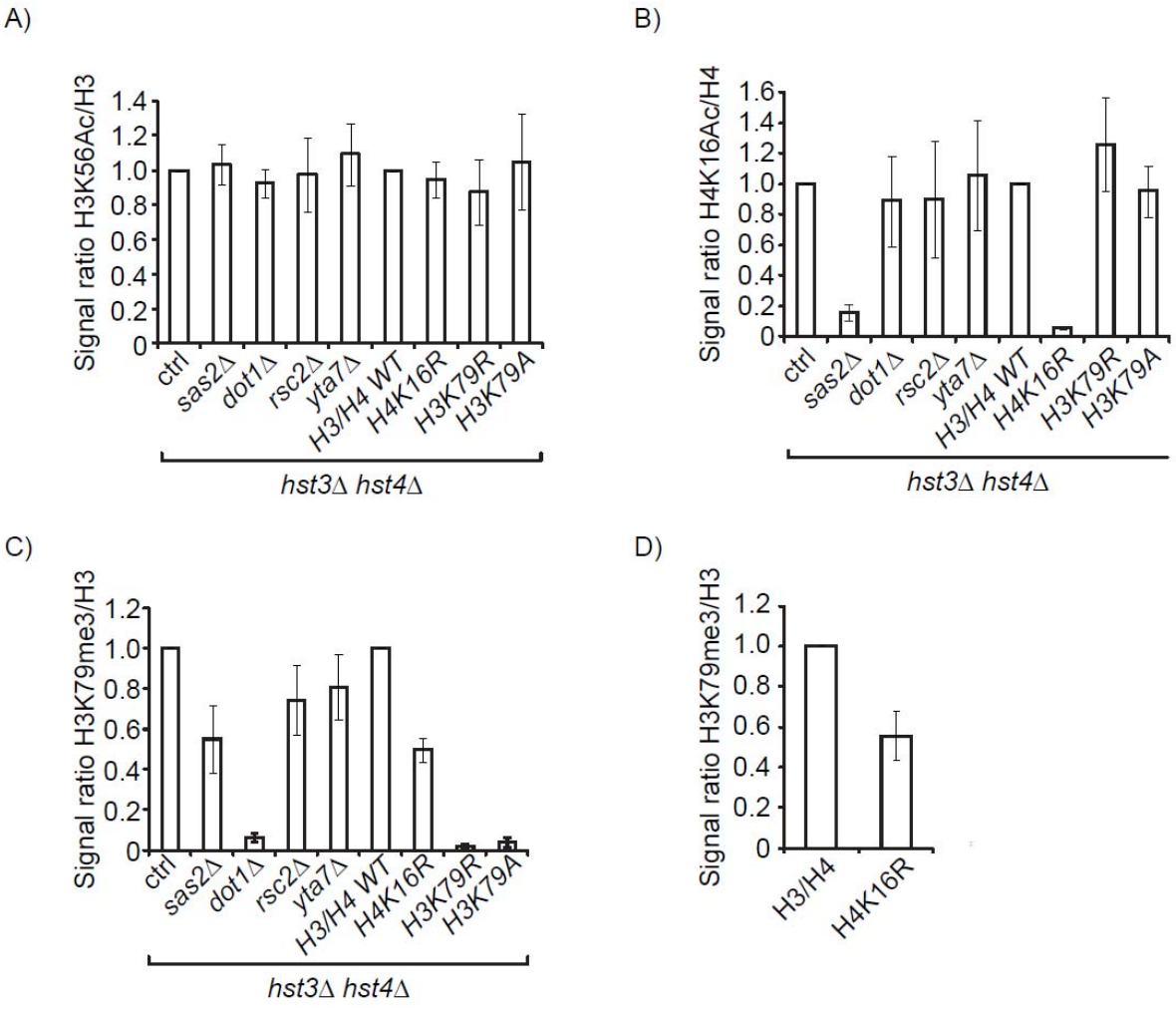

Figure S1 Densitometry analysis of immunoblots shown in Figure 4D and E**.** A-C) Immunoblot images from Figure 4D were analyzed by densitometry. Error bars represent the standard error of the mean of between 3 to 12 independent loadings of each sample. D) H3K79me3 immunoblot images from Figure 4E were analyzed by densitometry. Average values relative to the control signal derived from total histone H3 are shown and error bars indicate the standard error of the mean (from 4 independent loading of each sample).

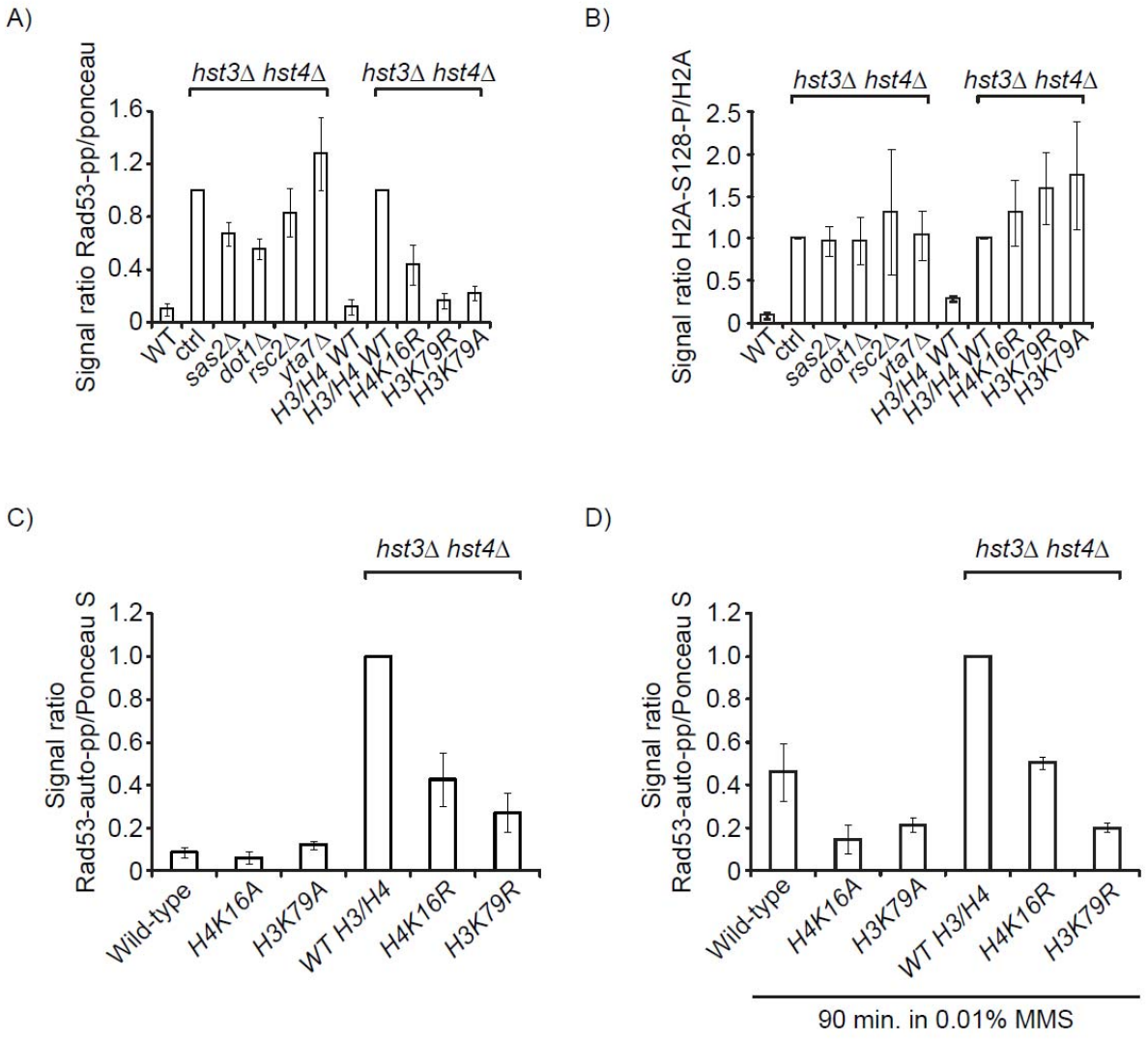

Figure S2 Densitometry analysis of immunoblots and Rad53 autophosphorylation assays shown in Figure 6B and 6C. A-B) Immunoblot or Rad53 autophosphorylation images from Figure 6B were analyzed by densitometry. Average signals relative to that observed in an isogenic *hst3*Δ *hst4*Δ strain are shown and error bars indicate the standard error of the mean (from at least 3 independent loadings of each sample).

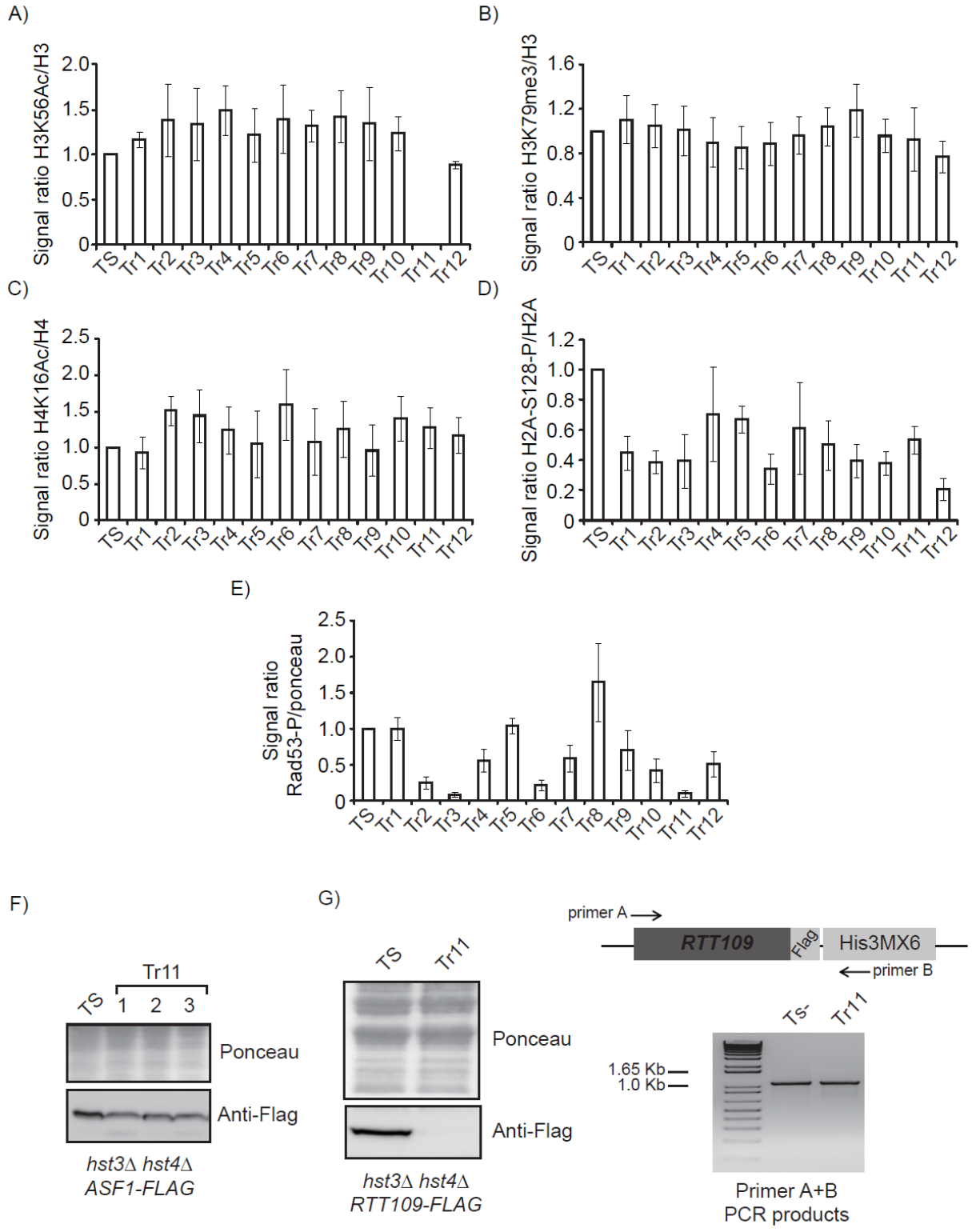
A)
Signal ratio H3K56Ac/H3
B)
Signal ratio H3K79me3/H3
C)
Signal ratio H4K16Ac/H4
D)
Signal ratio H2A-S128-P/H2A
E)
Signal ratio Rad53-P/ponceau
TS Tr1 Tr2 Tr3 Tr4 Tr5 Tr6 Tr7 Tr8 Tr9 Tr10 Tr11 Tr12
F)
Tr11
TS 1 2 3
Ponceau
Anti-Flag
hst3Δ hst4Δ
ASF1-FLAG
G)
TS Tr11
Ponceau
Anti-Flag
hst3Δ hst4Δ
RTT109-FLAG
primer A
RTT109
Flag
His3MX6
primer B
Ts- Tr11
1.65 Kb
1.0 Kb
Primer A+B
PCR products

Figure S3

Figure S3 Densitometry analysis of immunoblots and Rad53 autophosphorylation assays shown in Figure 7B. A-E) Immunoblots and Rad53 autophosphorylation images from figure 7B were analyzed by densitometry. The y-axes represent ratio of the signals obtained in each thermo-resistant strain (Tr) relative to the signal observed in the parental *hst3*Δ *hst4*Δ TS strain. Error bars indicate the standard error of the mean (at least 3 independent loading of each sample). F) Asf1 was epitope-tagged in the *Tr11* thermo-resistant spontaneous suppressor derived from *hst3*Δ *hst4*Δ Ts- mutant cells. Three independent clones derived from tagging Asf1 in the Tr11 strain were selected. Immunoblots of whole-cell lysates were probed to detect Asf1-Flag. Ponceau S staining is shown as loading control. G) The Rtt109-Flag protein is not detectable in the *Tr11* spontaneous suppressor of *hst3Δ hst4Δ* that lack H3K56Ac. Rtt109-Flag was detected by immunoblotting in whole-cell lysates of exponentially growing cells probed with a Flag antibody. (Right panel) Location of PCR primers used to ensure that DNA integration correctly resulted in an *RTT109-Flag* gene and PCR results showing that the *RTT109-Flag* gene is present in each of the strains analyzed for Rtt109-Flag protein expression in the left panel.

File S1

Supplementary Material and Methods

Histone purification, derivatization and mass spectrometry: Core histones were purified from yeast strains as previously described (GUILLEMETTE *et al.* 2011). Intact core histones were fractionated using an Agilent 1100 HPLC system equipped with a micro-fraction collector. Histone separations were performed using a ZORBAX 300SB-C8 column (5 µm, 300Å), 150×2.1 mm i.d. (Agilent Technologies), with a solvent system consisting of 0.1% trifluoroacetic acid (TFA) in water (v/v) (solvent A) and 0.1% TFA in acetonitrile (v/v) (solvent B). Gradient elution was performed from 5–90% B in 60 minutes at 150 µl/min. Fractions were collected in a 96-well plate at a rate of one fraction per minute. The fractions containing histone H3 were pooled and dried in a Speed-Vac concentrator. The dried samples were then subjected to propionylation to prevent internal cleavage of tryptic peptides lacking H3K56 acetylation or H3 peptides containing K79 that was either non-methylated or mono-methylated. Derivatization of intact histone H3 was conducted by adding a freshly prepared emulsion composed of 2:1 (v/v) water: propionic anhydride (Sigma), and vortexing for 1 h at room temperature. After the propionylation, samples were dried a second time, resuspended in 0.1 M ammonium bicarbonate, and digested overnight at 37°C using sequencing grade modified trypsin (Promega). The tryptic digests were dried to completion and resuspended in 0.2% formic acid in water (v/v) prior to mass spectrometry (MS) analysis. MS data were acquired in duplicate on a Q Exactive Plus mass spectrometer coupled to an EASY nLC II system (Thermo scientific). Peptides were first desalted on a Jupiter C18 (3-mm particles, Phenomenex) trap column (4-mm length, 360 mm i.d.) for 5 min at 10 µl/min, prior to their elution onto a C18 analytical column (18-cm length, 150 mm i.d.). A linear gradient from 5 to 60% acetonitrile (containing 0.2% formic acid) at 600 nl/min over 90 min was used for peptide elution. The MS instrument was operated in positive ion mode, and capillary voltage of 1.6 kV. MS scans were acquired in the Orbitrap analyzer over the range of 300 – 1500 *m/z* at a resolution of 70,000 and automatic gain control target value of 1.0×10^6. An inclusion list containing *m/z*, charge state and collision energy (CE) values of H3 peptides was used to trigger MS/MS acquisition. Every precursor ion found in the inclusion list was automatically selected for fragmentation in the HCD cell at a normalized CE setting of 27. The fragments were analyzed in the Orbitrap at a resolution of 35,000 and a target value of 5.5×10^5. The dynamic exclusion setting was disabled in order to acquire multiple MS/MS spectra per peptide. The relative abundance of peptides containing acetylated H3K56 or mono-, di- and tri-methylated H3K79 or their propionylated counterparts (corresponding to peptides that were not modified at K56 or K79 *in vivo*) was manually calculated from base peak intensities of extracted ion chromatograms.

H3K79me0, me1, me2 and me3: The percentages listed in Table 5 were calculated as follows. The relative abundance of H3 molecules lacking H3K79 methylation (K79me0) *in vivo* (expressed as percentage of all forms of the peptide containing K79),

was calculated as the abundance of the K79me0+pr peptide divided by the total abundance of the K79me0+pr, K79me1+pr, K79me2 and K79me3 peptides (where "pr" indicates *in vitro* propionylation). The same approach was employed to calculate the relative abundance of peptides containing H3K79me1, H3K79me2 and H3K79me3. *In vitro* propionylation can only occur on histone molecules that are non-methylated or mono-methylated *in vivo*; H3 molecules di- or tri-methylated *in vivo* cannot be propionylated. Hence, the percentages listed in Table 5 cannot be equated to stoichiometries because, after *in vitro* propionylation, the peptides with various degrees of methylation are chemically heterogeneous and, as a result, are not necessarily detected with the same efficiency (due to issues such as differences in charge and hydrophobicity affecting recovery from reversed phase HPLC and ionization/detection in the mass spectromer)(LIN *et al.* 2014).

H3K56ac stoichiometry: Because there is only one very abundant modification within the peptide containing K56, the percentages listed in Table 5 reflect stoichiometries of K56ac that were calculated as mentioned below. After *in vitro* propionylation, only two abundant tryptic peptides that differ by only one methylene group were detected: peptides derived from H3 molecules that lacked K56 acetylation *in vivo* (K56pr) and peptides that contained K56 acetylation *in vivo* (K56ac). Hence, the stoichiometry of H3K56 acetylation in each strain can be simply calculated as the abundance of the K56ac peptide divided by the total abundance of the K56ac and K56pr peptides. To ensure that K56ac stoichiometries were as accurate as possible, we also conducted two types of controls for the derivatization step. The first control was to ensure that *in vitro* propionylation proceeded with high efficiency. Inefficient propionylation of lysines that are not acetylated *in vivo* leads to overestimation of the stoichiometry of acetylation because peptides lacking lysine modification are cleaved by trypsin. The peptide that we monitored to determine the efficiency of propionylation was 57-STELLIR-63, which is generated by trypsin cleavage after a non-propionylated K56. Under our conditions, we estimated that a single round of propionylation led to an efficiency of H3K56 derivatization of 97.5%.

Second, it has been reported that, under certain conditions (*e.g.* multiple rounds of propionylation), propionylation can result in undesirable side reactions, such as O-propionylation of serine side chains (DROGARIS *et al.* 2008; LIAO *et al.* 2013). It is important to minimize these side reactions because peptides containing those modifications are chemically different from those containing only K56ac or K56pr and, therefore, difficult to take into account in calculations of acetylation stoichiometries. Under our conditions, we found that S57 propionylation occurred in roughly 6% of H3 moecules. Propionylation of H3-T58 was not detected. Based on this, we feel confident that undesirable H3-S57 or H3-T58 propionylation did not adversely affect our ability to determine H3K56Ac stoichiometries.

Supplementary references

DROGARIS P., WURTELE H., MASUMOTO H., VERREAULT A., THIBAULT P., 2008 Comprehensive profiling of histone modifications using a label-free approach and its applications in determining structure-function relationships. Anal. Chem. **80**: 6698–6707.

GUILLEMETTE B., DROGARIS P., LIN H.-H. S., ARMSTRONG H., HIRAGAMI-HAMADA K., IMHOF A., BONNEIL E., THIBAULT P., VERREAULT A., FESTENSTEIN R. J., 2011 H3 lysine 4 is acetylated at active gene promoters and is regulated by H3 lysine 4 methylation. PLoS Genet. **7**: e1001354.

LIAO R., WU H., DENG H., YU Y., HU M., ZHAI H., YANG P., ZHOU S., YI W., 2013 Specific and efficient N-propionylation of histones with propionic acid N-hydroxysuccinimide ester for histone marks characterization by LC-MS. Anal. Chem. **85**: 2253–2259.

LIN S., WEIN S., GONZALES-COPE M., OTTE G. L., YUAN Z.-F., AFJEHI-SADAT L., MAILE T., BERGER S. L., RUSH J., LILL J. R., ARNOTT D., GARCIA B. A., 2014 Stable-isotope-labeled histone peptide library for histone post-translational modification and variant quantification by mass spectrometry. Mol. Cell. Proteomics MCP **13**: 2450–2466.